ISSN: 2229-7359 Vol. 11 No. 15s,2025

https://theaspd.com/index.php

Computational Approach For Analyzing Resistance In Staphylococcus Aureus Against Aztreonam And Ceftazidime Contrasting Nonresistance **B**-Lactam Antibiotics

Viqar Agha¹, Mohini Chaurasia², Zeeshan Fatima³, Tanveer Ahamad⁴, Abdul Quddoos⁵Romi Singh⁶
^{1,2,6}Era College of Pharmacy, Era University, Sarfarazganj, Lucknow, 226003 (U.P) India.

Abstract: The contemporary landscape of drug design is witnessing a pronounced shift towards the utilization of dry lab, predominantly owing to the availability of robust and reliable software tools, coupled with the convenience of computational work. The primary objective of this study is to validate the efficacy of the in Silico (dry lab) approach for subsequent In vitro analysis. Our focus is to establish a correlation between the results obtained through the Antimicrobial Susceptibility Test (AST) using the disc diffusion method and the docking scores of, β -lactam and all drugs representing these antibiotic classes are known to interact with the same receptor, Penicillin-binding Protein (PBP).

To achieve this, we employed six different docking software tools, each utilizing distinct approaches for ligand-receptor interactions. These tools include Autodock Vina 4, Swissdock, Discovery Studio (CD Docker) for site-specific ligand binding to receptors, CB dock2 for blind docking, and Protein Plus and Patchdock, which are pocket-cavity-based docking algorithms. The results of our analysis reveal varying degrees of correlation between the docking scores and the AST results. Notably, a significant positive association was observed in Swissdock, followed by Discovery Studio (CD Docker), while Autodock Vina 4 demonstrated only a moderate association. The significance levels, as determined by p-values, were consistently below 0.05 in these instances.

In conclusion, our study underscores the necessity for standardization and harmonization among different docking software to ensure consistency in results. To enhance validation, we conducted molecular dynamics simulations spanning 100 nanoseconds each. This extensive timeframe allows for effective ligand-protein stabilization.MD simulation reveals RMSD value of ceftazidime (0.000493- 14.337) was the lowest among all β -lactam that's in agreement with In vitro results ceftazidime have zone of inhibition (zoi) nil. The RMSF value of aztreonam was (0.0562-0.8636) highest among all β -lactam, higher RMSF values suggest greater flexibility and possibly less stability in specific parts of the molecule. which matches with In vitro result zoi of aztreonam was nil.

Keywords: Molecular dynamics, Staphylococcus aureus Antibiotic Resistance, β -lactam, Docking.

Abbreviation: ZOI- Zone of Inhibition, ATCC American Type Culture and Collection, PBP- penicillin-binding proteins, MRSA-methicillin-resistant Staphylococcus aureus

1. INTRODUCTION

Antibiotics have revolutionized the field of medicine, offering effective tools in the fight against bacterial infections. However, the emergence of antibiotic-resistant pathogens poses a formidable challenge to public health [1]. Staphylococcus aureus, a notorious pathogen, has developed resistance to multiple antibiotics [2], necessitating the exploration of innovative therapeutic strategies. In this context, comparative docking studies of β -lactam antibiotics [3] against S. aureus can offer valuable insights into the molecular interactions between these drugs and their target proteins. β -lactam antibiotics, such as penicillin, cephalosporins, and carbapenems are among the most widely used classes of antibiotics. They exert their bactericidal effect by inhibiting the bacterial cell wall synthesis [4], primarily through binding to penicillin-binding proteins (PBPs). Staphylococcus aureus [5], a Gram-positive bacterium, is a significant causative agent of skin and soft tissue infections, septicemia [6], and a variety of other clinical conditions. The emergence of methicillin-resistant Staphylococcus aureus (MRSA) strains [7], which often display resistance to multiple antibiotics, highlights the need for a comprehensive understanding

³Amity Institute of Pharmacy, Lucknow, Amity University Uttar Pradesh Lucknow, India, Sector 125, Noida, 201313, India.

⁴Department of Biotechnology, Era University, Sarfarazganj, Lucknow, 226003(U.P) India.

⁵Department of Liberal Education, Era University, Sarfarazganj, Lucknow, 226003(U.P) India.

ISSN: 2229-7359 Vol. 11 No. 15s,2025

https://theaspd.com/index.php

of the interactions between antibiotics and their target sites.

This research paper endeavors to bridge the gap between In vitro and $in\ Silico$ approaches to understand the efficacy of β -lactam and carbapenem antibiotics against S. aureus. In vitro studies involve laboratory experiments where the zone of inhibition is measured to determine the antibacterial activity of these antibiotics [8]. However, these experiments do not provide detailed insights into the molecular mechanisms underlying their activity. In contrast, $in\ Silico\ docking\ studies\ utilize\ computational techniques to predict the binding affinity and interactions between antibiotics and their target proteins. These studies can provide valuable information regarding the specific residues involved in binding and potentially aid in designing novel antibiotics with improved efficacy [9].$

This study also aims to establish a predictive relationship between the Zone of Inhibition (ZOI) and docking scores [10], operating under the assumption that there exists a direct correlation between the ZOI and the docking scores of antibiotics [11]. We posit that the binding of ligands with their respective receptors serves as the primary determinant in elucidating the response or vice versa [12], thereby suggesting that ZOI represents a measure of binding affinity

Intriguingly, the competitive inhibitory interaction between Penicillin-binding Protein (PBP) and antibiotics adheres to Michaelis-Menten kinetics [13]. The substrate concentration at which the velocity reaches half-maximum (1/2 Vmax) is referred to as the Km (or Ki for inhibition) value, denoted in units of moles per liter (M). It is important to note that the binding affinity of a substrate to an enzyme exhibits an inverse relationship with Km and Ki values [14]; the higher the affinity, the lower the Km or Ki value. This study seeks to explore the precision and accuracy of *in Silico* methodologies in predicting In vitro outcomes within biological systems [15]. In this pursuit, we aim to discern the extent of our capabilities and confront the limitations inherent in *in Silico* models utilizing various computational methodologies. These methodologies encompass Autodock Vina [16], Patch Dock [17], Swissdock [18], Protein Plus [19], CB-Dock [20], and Discovery Studio [21]. For this investigation, the receptor of interest is Penicillin-binding Protein 2b [22] (PBP) of Staphylococcus aureus [23] ATCC No-25923. The protein structure was constructed using the Swiss Model [24], and we consider ten antibiotics in our study: The selection of ten antibiotics aimed to generate a substantial dataset, enabling comprehensive statistical analysis [25] both In vitro and *in Silico*

Through these efforts, we aspire to refine our understanding and prediction capabilities in the realm of antibiotic responses by including molecular dynamics. This study further aims to contribute the data which may help to the development of more effective antibiotics and strategies for combatting antibiotic-resistant bacteria. Such research has the potential to benefit both patients and healthcare systems, ultimately helping to mitigate the growing threat of antibiotic resistance [1]

2. MATERIAL AND METHODS

Staphylococcus aureus ATCC No-25923 strains were sourced from Era Medical College's Microbiology laboratory, which is affiliated with Era University in Lucknow, Uttar Pradesh, India. These strains were maintained as stock cultures within a Microbank, with cryovials stored at -80°C until they were needed for use. The Nutrition Agar media [26] used in the experiments was procured from the Microbiology department at Era University.

For the antibiotic sensitivity testing, we employed antibiotic disks including Cefotetan (30 μ m), Cefoperazone (75 μ m), Ceftazidime (30 μ m), Cefixime (30 μ m), Cefepime (30 μ m), Meropenem (10 μ m), Imipenem (10 μ m), Doripenem (10 μ m), Aztreonam (30 μ m), and Ertapenem (10 μ m), all of which were obtained from Hi Media.

In our In vitro experiments, we focused on Staphylococcus aureus ATCC No-25923 as our microorganism of choice [27]. Its DNA and protein sequences were retrieved from the ATCC website (https://www.atcc.org/products/25923) (table 1). Specifically, we obtained the protein sequence consisting of 527 amino acids for Penicillin-binding protein 2b in Staphylococcus aureus ATCC No-25923 from the ATCC website. This approach ensured the integrity of our microbial cultures and the accuracy of the genetic and protein information utilized in our study.

ISSN: 2229-7359 Vol. 11 No. 15s,2025

https://theaspd.com/index.php

Table 1: Genetic information of Penicillin binding protein 2b Staphylococcus aureus

Sequence Start Sequence End		Gene Id	Name of protein		
2034628	2036824	PbpB	Penicillin Binding Protein 2 B		

Bacterial Culture

Prior to conducting the sensitivity testing, Staphylococcus aureus ATCC No25923 was cultivated on a nutrient agar plate and subsequently incubated for duration of 24 hours at a temperature of 37°C. From this culture, a single colony was selected and propagated in 5 ml of liquid peptone media for a period of 4 hours, again at a temperature of 37°C [28].

To ensure consistency in the density of the culture required for the testing process, adjustments were made to achieve a measurement of 0.5 McFarland standards, corresponding to 1.0x10^8 CFU/ml, which was assessed using a Turbidimeter (LB-966 Moglix) [29]

Disc Diffusion Method

Antimicrobial susceptibility testing was conducted in accordance with the standard disc diffusion method. Staphylococcus aureus cultures, maintained at a density of 0.5 McFarland standard [30], were evenly spread onto Nutrition agar plates using a sterile swab. These plates were allowed to air dry for a duration of 15 minutes before the initiation of the sensitivity testing [30].

Subsequently, antibiotic discs, including Cefotetan (30 μ g), Cefoperazone (75 μ g), Ceftazidime (30 μ g), Cefixime (30 μ g), Cefepime (30 μ g), Meropenem (10 μ g), Imipenem (10 μ g), Doripenem (10 μ g), Aztreonam (30 μ g), and Ertapenem (10 μ g), were placed onto the agar plates in triplicate.

Following the placement of antibiotic discs, the plates were incubated at a temperature of 37°C for a period of 24 hours. Subsequently, the plates were examined in triplicate to determine the Zone of Inhibition, a key parameter in the assessment of antibiotic susceptibility.

Protein Modeling

Protein modeling plays a pivotal role in research on *in Silico* antibacterial resistance. By utilizing computational techniques and molecular modeling, scientists can predict how antibiotics interact with bacterial proteins, such as penicillin-binding proteins, and how mutations within these proteins can lead to resistance. These models help elucidate the molecular mechanisms behind antibacterial resistance, guiding the design of novel drugs and treatment strategies. Furthermore, protein modeling allows researchers to explore various scenarios and understand the impact of structural changes on the effectiveness of antibiotics, providing valuable insights into combating bacterial resistance in a rapidly evolving microbial landscape.

Protein modeling was conducted using the Swiss Model [31] platform (https://swissmodel.expasy.org/interactive). Initially, a suitable template was identified, and subsequently, the target protein sequence was aligned with the chosen template. Finally, the model of the protein was constructed. To ensure the accuracy and quality of the constructed model, validation was carried out using the Molprobity [32] (Table 2) (http://molprobity.manchester.ac.uk/).

Protein structure Preparation:

The protein model of Penicillin-binding Protein Subunit 2b from Staphylococcus aureus ATCC No 25923 was generated using Discovery Studio Visualizer version V2021.20.298 [33]. The docking input files were created by incorporating nonpolar hydrogen atoms into the PDB format. To ensure structural stability, energy minimization was carried out using the Swiss PDP [24] viewer, and the resulting file was saved in PDB format. For molecular docking investigations, multiple software tools were employed, including the Swissdock [34] online server, Autodock Vina [35] version 1.2.0, Protein Plus (JAMDA) [19], CB Dock2 [36], Discovery Studio[21], and the Patchdock [37] online server. This comprehensive approach facilitated a thorough analysis of ligand-receptor interactions in the context of antibacterial resistance research.

Molecular Docking

Receptor

A single binding protein was carefully selected and modeled utilizing the Swiss Model. In this process, the coordinates of the binding site, denoted as (x, y, and z), remained fixed [38]. These coordinate values were specified as -1.0615 (x), -8.069 (y), and 3.6761 (z). Additionally, the grid size remained constant at

ISSN: 2229-7359 Vol. 11 No. 15s,2025

https://theaspd.com/index.php

70 Angstrom for most tools, except in the case of blind docking tools like CB Dock2 and Patchdock.

Ligand

All the ligands are retrieved as per the requirement of Docking programs form Zinc database [39] and Pubchem database (https://pubchem.ncbi.nlm.nih.gov/). When a ligand shares the same receptor and demonstrates a similar mechanism of action In vitro across all docking parameters, it signifies a high degree of specificity and affinity between the ligand and the receptor [14]. This implies that the ligand efficiently interacts with the receptor, forming stable complexes, and ultimately triggers a consistent biological response [8]. In this scenario, the ligand is more likely to exhibit reliable and predictable effects on the receptor, making it a valuable tool in drug design and development. The consistency across docking parameters suggests that the ligand-receptor interaction is robust and dependable, which is critical for the development of therapeutic agents and understanding the molecular basis of various biological processes. It is essential for researchers and pharmaceutical scientists to explore such ligand-receptor interactions to harness their potential in the development of targeted therapies and better understand the intricacies of molecular recognition In vitro [10]

Molecular dynamics

Using GROMACS software (version 2023.2-MODIFIED) [40] on the Linux operating system46, we ran 100 ns MD simulations of protein-ligand complexes that were identified by molecular docking. The CHARMM36 force field was used to create the protein topologies [41] the swissparam server were used to generate the ligand topology with CHARMM36 force field [42], and each system was dissolved using the TIP 3-point solvent model, and the charge was subsequently neutralized using the proper concentrations of Na+ and Cl—. The system energy was minimized using the steepest descent minimization algorithm, which halted at > 50,000 steps and a maximum force of < 10.0 kJ/mol. For every complex system, we carried out the NVT and NPT equilibration (1 bar pressure and 300 K temperature) [43]. The Fourier transform and the Particle Mesh Ewald were used to handle the long-range electrostatics. Here was 0.16 transform grid spacing. The MD simulation lasted 100 ns, with a time step of 2 fs and a structural coordinate saving frequency of 10 ps. We assessed a number of MD metrics, including RMSD and Root Mean Square studies on hydrogen bonding (H-bond) and fluctuation (RMSF) [44]. Furthermore, the non-bond interaction energies between ligands and proteins, such as van der Waals and short-range electrostatic interactions (Vdw) were furthermore computed.

Statistical Tool

The data analysis for this study was conducted using two powerful open-source statistical software tools, PSPP [45] and R [46]. PSPP, developed by the Free Software Foundation, is a user-friendly application for performing various data manipulation, visualization, and statistical analyses. It provides a range of essential functions for data processing and is particularly useful for researchers who prefer an open-source alternative to commercial statistical software. R, on the other hand, is a widely acclaimed and versatile programming language and environment for statistical computing and graphics. It offers an extensive array of statistical and graphical techniques and allows for custom scripting and analysis. By utilizing both PSPP and R in the data analysis process, researchers can benefit from a combination of user-friendly, point-and-click interfaces along with the advanced capabilities and flexibility that R provides, ultimately enabling a comprehensive and robust analysis of the research data.

3. RESULTS AND DISCUSSION

Penicillin-binding protein 2b (PBP2b) Fig 1 domains serve crucial roles in peptidoglycan metabolism [47], functioning as carboxypeptidases or transpeptidases. These domains are particularly vital for the growth and survival of Staphylococcus aureus [2]. In our modeling process, we selected the Crystal structure of Penicillin-Binding Protein 1 (PBP1) from Staphylococcus aureus complexed with pentaglycine fig2, as the most suitable template for PBP2b. The Qualitative Model Energy Analysis (QMEAN) Z-Score for the modeled protein [48] was -0.83, Fig 3 and Fig 4 indicating a reasonably reliable model. Local quality estimation Fig 5, revealed that amino acid sequences between positions 200 and 240 exhibited a lower level of structural quality, likely due to a predicted local similarity to the target that was below 0.6 [48]. Fortunately, the binding site coordinates did not fall within this lower-quality structural region, ensuring the reliability of the binding site in the model.

ISSN: 2229-7359 Vol. 11 No. 15s,2025

https://theaspd.com/index.php

Ramchandran Plot

Following the homology modeling, energy minimization was carried out to optimize the protein structure. Subsequently, the protein underwent a validation process. In the Molprobity analysis (Tab2), ProteinvalidationofPBP2bbyMolprobity, it was observed that 502 residues, accounting for 95.62% of the total, fell within the favored region, indicating a highly stable and favorable protein structure. Additionally, 438 residues (98.67%) were identified as having favored rotamers, further confirming the reliability of the protein model. Ramachandran outliers were minimal, with only 2 residues (0.38%) falling outside the expected range, suggesting a structurally sound model. The Rama distribution-Z Score was -0.59 ± 0.33 (Fig6), providing additional evidence of the overall quality and accuracy of the protein structure.

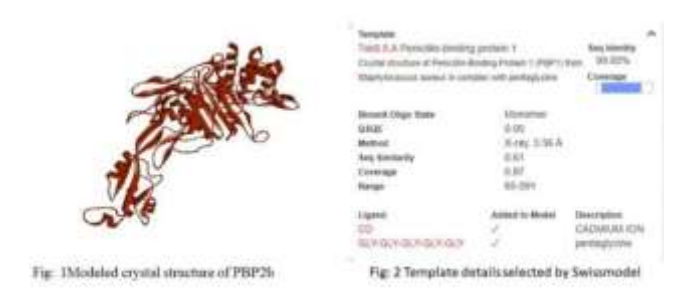


Figure 1. Represents the 3D structure of penicillin binding protein and Figure 2. Shows the templet details Sequence coverage and crystal state, ligand attached, selected by Swissmodel.

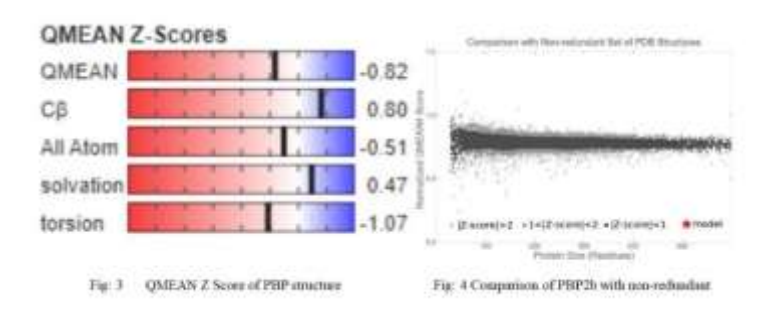


Figure 3 QMEAN Z-Score: 0.82. A QMEAN Z-score suggests that the model is somewhat less accurate than the average PDB structure but is still within an acceptable range. 0.8 C β score is a strong indicator that the modelling of the side-chain orientations and C β atom placements is quite reliable, contributing positively to the overall quality of the protein structure. All Atom: 0.51 Slightly negative, meaning that the atomistic model isn't perfectly ideal but still fairly reasonable. Solvation: 0.47Positive solvation energy indicates that the solvation interactions are modeled well, contributing positively to the overall structural reliability. Figure 4. The red star represents your protein model, and it falls within the Z-score range of |Z-score| < 1, indicating that it is comparable to other well-resolved protein structures.

Table 2: Protein Validation of PBP2b by Molprobity

	Poor rotamers	36	8.11%	Goal: <0.3%
	Favoured rotamers	373	84.01%	Goal: >98%
	Ramachandran outliers	6	1.14%	Goal: <0.05%
Protein	Ramachandran favoured	494	94.10%	Goal: >98%
Geometry	Rama distribution Z-score	-1.51 ± 0.33		Goal: abs (Z score)
				< 2
	Cβ deviations >0.25Å	9	1.88%	Goal: 0
	Bad bonds:	4 / 4249	0.09%	Goal: 0%
	Bad angles:	51 / 5715	0.89%	Goal: <0.1%

ISSN: 2229-7359 Vol. 11 No. 15s,2025

https://theaspd.com/index.php

Peptide Omegas	Cis Prolines:	2 / 25	8.00%	Expected: ≤1 per
				chain, or ≤5%
Low-resolution	CaBLAM outliers	13	2.5%	Goal: <1.0%
Criteria	CA Geometry outliers	6	1.15%	Goal: <0.5%
Additional	Tetrahedral geometry outliers	1		
validations				

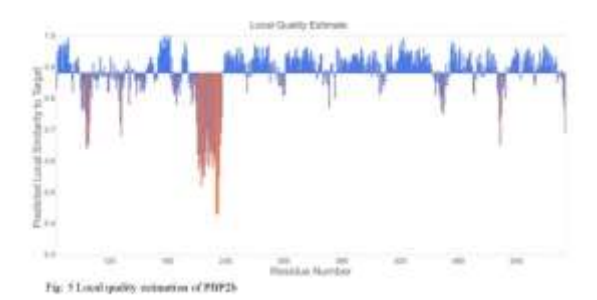


Figure 5. Local Quality Estimation of PBP2b X-axis (Residue Number): Represents the residue positions in the PBP2b sequence (from residue 0 to around 560). Y-axis (Predicted Local Similarity to Target): This scale ranges from 0.3 to 1.0, indicating how well the predicted structure aligns with a reliable target model. Values near 1.0 indicate high similarity (good local structural quality). Values below 0.7 suggest regions where the predicted structure may have poorer quality. There are significant drops around residues 220-260 (in orange/red), where the local quality dips below 0.6, with some regions close to 0.4. This suggests that the protein structure is not well-predicted in this region.

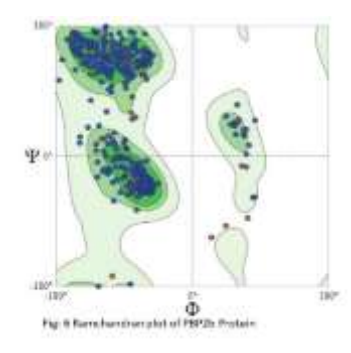


Figure 6. The Ramachandran plot for the PBP2b protein shows that the majority of the backbone torsion angles are in allowed and favored regions, indicating that the structure is generally well-modeled. The few outliers (red dots) may require closer inspection to understand whether they represent real structural features or issues with the model that need further refinement. However, the overall quality of the backbone geometry appears to be solid.



Figure 7. The image represents the structural and functional analysis of the protein PBP2B, as shown through the InterPro database. It consists of several annotated regions, each describing different aspects

ISSN: 2229-7359 Vol. 11 No. 15s,2025

https://theaspd.com/index.php

of the protein structure and associated domains, superfamilies, and features: Domains: The "PBP dimer" domain is represented as a purple bar, indicating a region involved in the dimerization of penicillin-binding proteins. This is crucial for their function. "PCN-bdTppet" (Transpeptidase domain) is in brown, highlighting a region responsible for the transpeptidase activity, which is critical in peptidoglycan biosynthesis. Homologous Superfamily: A green bar labelled "Beta lactam/transpeptidase-like" indicates a structural superfamily associated with transpeptidase activity, commonly found in beta-lactamase enzymes, suggesting that PBP2B has similar structural and functional properties. The brown "PBP dimer sf" marks the dimerization domain at a broader level within the superfamily context. Unintegrated Features: A long pink bar titled "PEPTIDOGLYCAN D, D-TRANSPEPTIDASE" refers to the unintegrated region, showing PBP2B's involvement in the enzymatic activity essential for bacterial cell wall synthesis.

Table 3: Post docking Results with zoi

S.n o	Drugs	Zone of In hibiti on in mm	Autodoc k Binding affinity	Swiss dock Bindi ng affinit y	Protei n Plus bindin g affinit y	Patchdoc k binding affinity	CB dock2 bindin g affinit y	Discover y Studio CD Score binding affinity
1	Cefotetan	22	-7.4	-9.02	1.728	5936	-7.5	41.013
2	Cefixime	17	-7.9	-9.11	1.865	5424	-7.9	-24.8303
3	Cefepime	16	-7.2	-8.59	2.2107	6212	-8	-4.43041
4	Ceftazidime	Nil	-7.3	-6.9	2.5392	6136	-8.3	-22.7362
5	Cefoperazon e	27	-9	-8.7	2.607	6042	-8.8	5.02232
6	Meropenem	32	-7.7	-9.02	1.79	4492	-7.8	18.8021
7	Doripenem	35	-8	-9.71	2.63	5006	-7.9	3.41344
8	Imipenem	27	-6.9	-8.91	1.757	4188	-6.8	11.0485
9	Ertapenem	30	-9.1	-9.72	2.836	5206	-9.3	14.6171
10	Aztreonam	Nil	-7.7	-8.72	.634	4798	-7.9	-18.9221

Table4: Ranking tally statistical rank of docking scores was generated by R statistical tool

Rank s of ZOI	Drug	ZOI in mm	Ranks of Swissdoc k	Ranks Of Discov ery Studio	Ranks Of Patchdoc k	Ranks Of Autodoo k	Ranks Of protei n plus	Rank s of CB dock
1	Doripenem	35	2	6	7	3	3	6
2	Meropenem	32	6	2	9	5	8	8
3	Ertapenem	30	1	3	6	1	1	1
4.5	Cefoperazon e	27	8	5	3	2	4	2
4.5	Imipenem	27	4	4	10	10	9	10
6	Cefotetan	22	5	1	4	7	10	9
7	Cefixime	17	3	10	5	4	7	5
8	Cefepime	16	9	7	1	9	6	4
9.5	Ceftazidime	0	10	9	2	8	5	3
9.5	Aztreonam	0	7	8	8	5	2	7

Protein Ligand Interaction/ comparative Rank and scores

ISSN: 2229-7359 Vol. 11 No. 15s,2025

https://theaspd.com/index.php

Cefotetan

The interaction between Cefotetan [49] and the penicillin-binding protein, as depicted in Fig8, revealed specific interacting amino acids. Notably, Thr309 and Ser426 engaged in conventional hydrogen bonding, while Ala520 and Ser527 formed interactions through pi donor hydrogen bonding and pialkyl bonding (Fig8). In vitro susceptibility studies were conducted using the disc diffusion method, yielding an average Zone of Inhibition (ZOI) of 22mm ± 0.2mm, falling within the effective range [49]

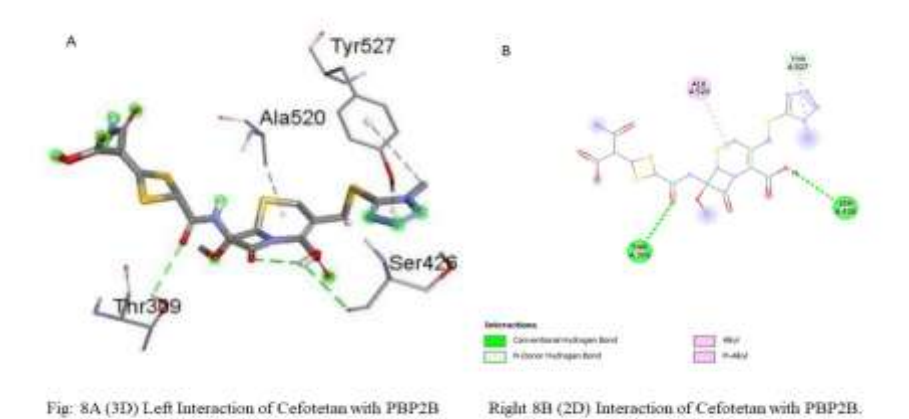


Figure 8A. Figure 8A (3D Interaction) The left panel shows a 3D view of the interaction between Cefotetan and PBP2B. Several key residues of PBP2B, such as Thr309, Ala520, Tyr527, and Ser426, are labeled, indicating points of interaction. Green dashed lines represent hydrogen bonds formed between the antibiotic and specific amino acids in PBP2B, like Ala520 and Ser426. These interactions stabilize the binding of Cefotetan to the protein. The spatial structure helps visualize the proximity of the drug to various amino acids and its orientation in the binding pocket of PBP2B. Figure 8B (2D Interaction) The right panel shows a 2D diagram of the same interaction, highlighting different types of chemical interactions between Cefotetan and PBP2B. Green dashed lines denote conventional hydrogen bonds. Pink dashed lines denote Pi-donor hydrogen bonds, which involve aromatic ring interactions contributing to binding affinity. Other interaction types, such as alkyl and Pi-alkyl interactions (highlighted in purple and pink), show how non-polar portions of the drug are involved in stabilizing the binding. Important amino acids such as Ala520 and Tyr527 are involved in these interactions, supporting the 3D representation from the left panel.

In terms of binding affinity, Autodock recorded a score of -7.4, Swissdock scored -9.02, Protein Plus yielded 1.728, and Patch Dock resulted in a score of -5936. The ranking of Cefotetan varied across different methods, with ZOI hierarchy positioning it 6th (Tab3). Autodock Vina and Swiss Dock ranked it 7th and 5th, respectively (Tab4), while Protein Plus placed Cefotetan at the bottom, 10th position. On the other hand, Patch Dock ranked Cefotetan 4th, CB-Dock2 placed it 9th (Tab4), and Discovery Studio with a CD Score of 41.03 awarded the top position to Cefotetan, indicating some discrepancies in the rankings according to different docking and inhibition methods.

Cefexime

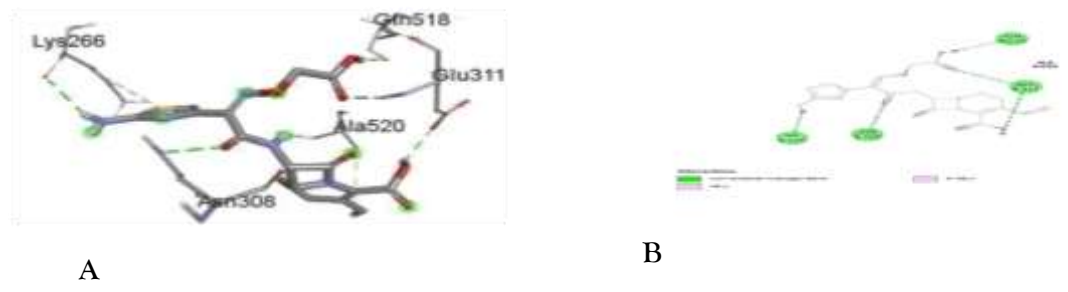


Fig: 9A (3D) Left Interaction of Cefixime with PBP2B, right 9B (2D) Interaction of Cefixime with PBP2B.

ISSN: 2229-7359 Vol. 11 No. 15s,2025

https://theaspd.com/index.php

Cefixime, an oral cephalosporin antibiotic, stands out due to its resistance to common plasmid-mediated enzymes and beta-lactamases, which are typically responsible for deactivating oral penicillin cephalosporins [50]. Figure 9 reveals the specific interactions of Cefixime with PBP [51], forming hydrogen bonds with Lys266, Asn308, Glu311, and Gly518, while also engaging with Ala520 through Pi Alkyl and Alkyl bonding. In terms of its antibacterial effectiveness, Cefixime demonstrates a moderate impact against Staphylococcus Aureus ATCC No 25923, displaying an average zone of inhibition measuring approximately 17mm±0.1mm.

In the realm of *in Silico* binding affinity assessments, various calculations yield distinct results: AutoDock Vina reports a score of -7.9, SwissDock records -9.11, Protein Plus calculates 1.865, Patchdock arrives at 5424, and CB Dock2 reports -7.9. When ranked according to the descending order of zone of inhibition (ZOI) effectiveness, Cefixime secures the 7th position, while AutoDock Vina places it in 4th, and SwissDock positions it in 3rd place. Protein Plus corroborates its 7th place ranking in line with its ZOI performance. Patchdock and CB Dock2 both assign Cefixime the 5th position. However, it is noteworthy that Discovery Studio yields a substantially lower score of -24.8303, placing Cefixime in the bottom 10 positions. This disparity in rankings highlights the complexities involved in evaluating drug interactions and efficacy, underscoring the necessity of employing multiple approaches to comprehensively assess drug candidates.

Cefepime

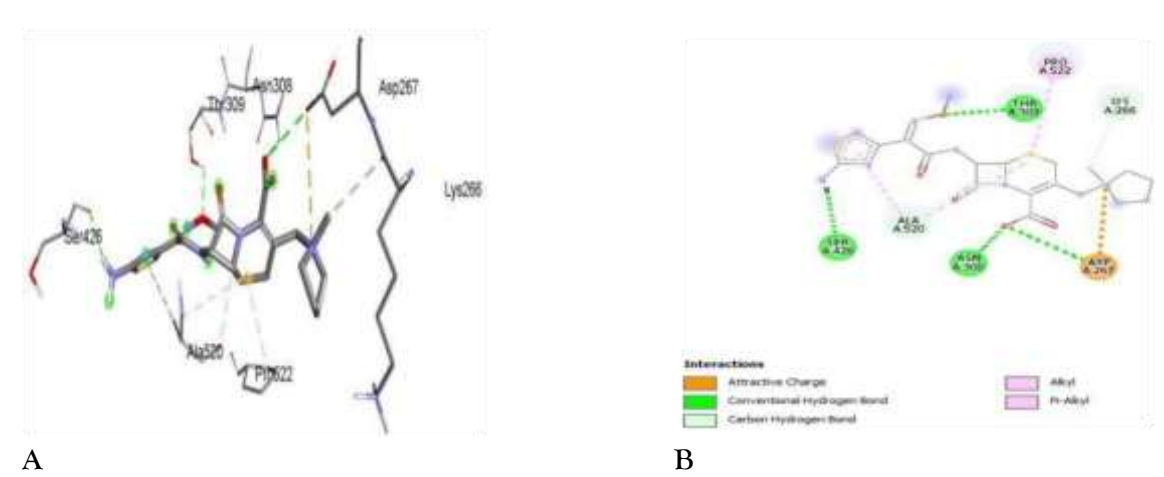


Fig: 10A (3D) Left Interaction of Cefepime with PBP2B, right 10B (2D) Interaction of Cefepime with PBP2B.

Cefepime, classified as a fourth-generation cephalosporin, boasts a wide-ranging antibacterial spectrum of action [52]. In Figure 10, it's evident that cefepime establishes significant interactions with Asn 308, Ser 426, and Thr 309 through conventional hydrogen bonding, while Ala 520 engages via pi Alkyl bonding and Pro 522 Lys 266 through Alkyl bonding. Its average zone of inhibition (ZOI) is measured at 16 ± 1 mm, which places it as the lowest-ranked contender in sensitivity testing, holding the 8th position based on ZOI.

When considering *in Silico* binding affinity calculations, the following scores emerge: AutoDock: -7.2, Swiss Dock: -8.59, Protein Plus: 2.2101, Patchdock: 6212, and CB Dock2: -8. AutoDock ranks cefepime at the 9th position, Swiss Dock situates it at the 8th position, and Protein Plus positions it at the 6th place, aligning with AutoDock's assessment. However, Patchdock significantly diverges from the other methods by ranking cefepime in the 1st position with the highest score of 6221. CB Dock places cefepime in the 4th position with a score of -8, and Cefepime secures the 7th position with a score of -4.4034 in Discovery Studio. This variability in rankings underscores the intricacies of evaluating drug interactions and efficacy, highlighting the importance of employing multiple assessment methods to gain a comprehensive understanding of potential drug candidates.

ISSN: 2229-7359 Vol. 11 No. 15s,2025

https://theaspd.com/index.php

Ceftazidime

Ceftazidime is classified as a 3rd generation cephalosporin, demonstrating resistance against Staphylococcus Aureus while effectively targeting gram-negative bacteria[47], as illustrated in Figure 11. Interestingly, In vitro assessments reveal a complete absence of any zone of inhibition (ZOI), indicating no observed activity. In stark contrast, *in Silico* analysis conducted with various binding software tools paints a different picture. In these simulations, Ceftazidime interacts with amino acids such as Thr309, Ser426, Glu311, Ser556, and Asn308, forming conventional hydrogen bonds, as well as engaging Ala520 through pi Alkyl bonding.

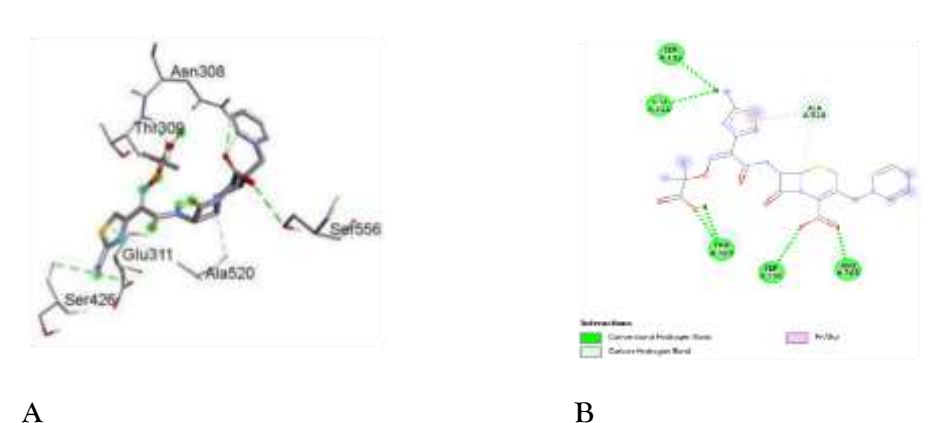


Fig: 11A (3D) Left Interaction of Ceftazidime with PBP2B, Right 11B (2D) Interaction of Ceftazidime with PBP2B.

In the hierarchy of effectiveness based on ZOI, Ceftazidime occupies the last position, with no observable ZOI. However, the results from various *in Silico* tools vary. AutoDock Vina ranks Ceftazidime 8th with a docking score[53] of -7.3, Swiss Dock places it in the 10th position with a docking score of -6.9, and Protein Plus Server surprisingly positions Ceftazidime 5th with a score of 2.5392. In stark contrast, PatchDock places Ceftazidime 2nd in rank with a score of 6136, while CB Dock2 positions it in 3rd place with a binding affinity score of -8.3. Discovery Studio, on the other hand, ranks Ceftazidime second to last, at 9th place, with a score of -22.7362. The variations in these assessments underscore the complexity of evaluating drug interactions and emphasize the importance of utilizing multiple assessment methods to gain a comprehensive understanding of potential drug candidate

Cefoperazone

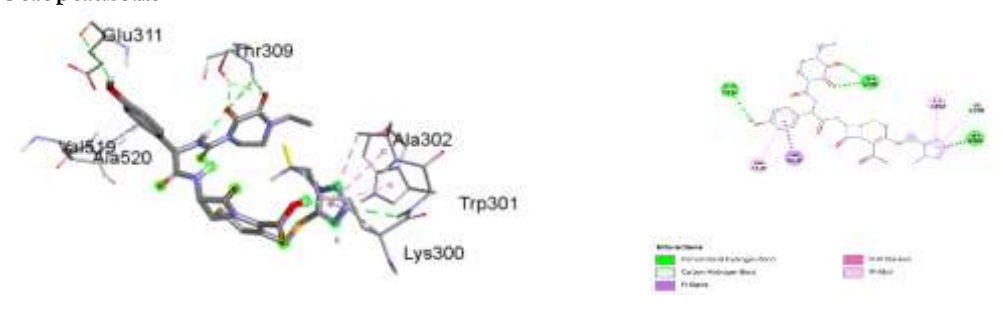


Fig: 12A (3D) Left Interaction of Cefoperazone with PBP2B, right 12B (2D) Interaction of Cefoperazone with PBP2B.

Cefoperazone, classified as a third-generation cephalosporin, demonstrates a wide-ranging antimicrobial spectrum, effectively combating both gram-positive and gram-negative aerobic and anaerobic [54] microorganisms. In Figure 12, the interaction of Cefoperazone with penicillin-binding protein (PBP) reveals significant bonds with Glu311, Thr309, Trp301, forming hydrogen bonds, as well as interactions with Ala520 and Ala302 through pi alkyl bonding, Lys300 via carbon-hydrogen bonding, and Val519

ISSN: 2229-7359 Vol. 11 No. 15s,2025

https://theaspd.com/index.php

forming pi sigma bonds. Notably, the average zone of inhibition (ZOI) measures 27mm±1mm, highlighting its remarkable effectiveness.

Aztreonam

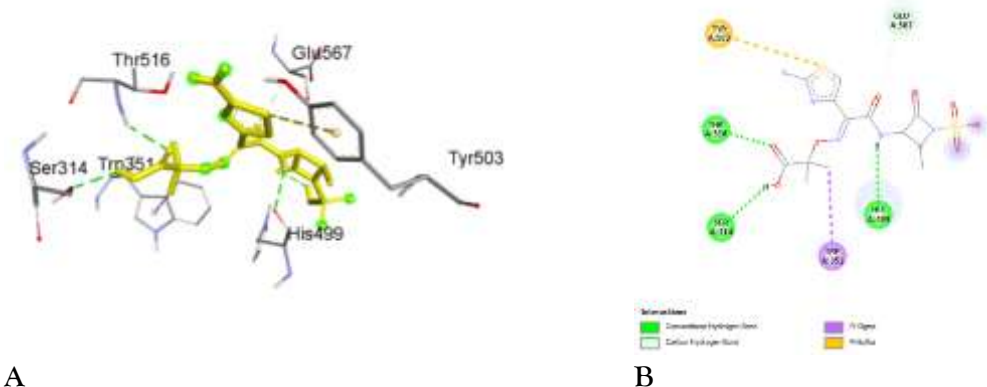


Fig: 13A (3D) Left Interaction of Aztreonam, with PBP2B,

right 13B (2D) Interaction of Aztreonam with PBP2B.

protein plus ranks Aztreonam in 2nd position with a score of 2.634 and Patchdock places Aztreonam in 8th position with a score of 4798 in close proximity to Swiss dock, interestingly Aztreonam was ranked at 5th position along with cefixime and Doripenem with a common score of -7.9 while Discovery studio ranks Aztreonam to 8th position with CD Dockers score of -18.9221. It's a broad-spectrum carbapenem anti-antimicrobial agent with a narrow spectrum of activity and a long plasma half-life39. Ertapenem Ranks 3rd in position according to descending order of ZOI Hierarchy with an average zone of inhibition of 27mm ± 1mm Fig 17 Thr516, Arg353 forms hydrogen bonds, Leu416 forms alkyl bonds, where Trp315 forms pi- pi stacked bonds with a benzene ring and Asn370 forms unfavorable Donor-Donor interaction, Auto dock vina scores -9.1 and ranks 1st i.e. in an agreement to In vitro results, Swiss dock ranks Ertapenem to 1st position very precise with *in Silico* and In vitro results and give the highest score of -9.72 among all under Swiss dock parameters, protein plus also places Ertapenem to 1st position accurately with Swiss dock and auto dock and give a maximum score of 2.836 in comparison to other docking platforms Patchdock ranks Ertapenem to 6th position with a score of 5206, CB Dock Confirms no1 rank of Ertapenem with the highest score of -9.3. Discovery Studio scores 14.6171 with 3rd position.

Meropenem

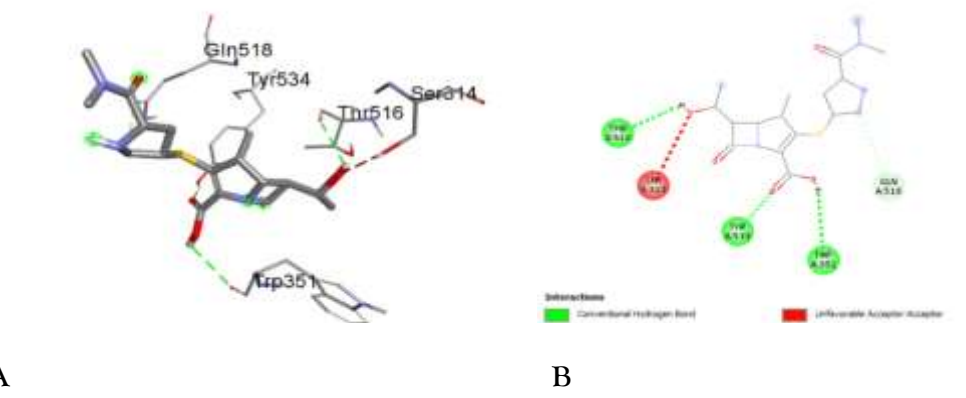


Fig: 14 A(3D) Left Interaction of Meropenem with PBP2B, right 14B (2D) Interaction of Meropenem with PBP2B.

Meropenem, classified within the carbapenem class, demonstrates efficacy against a broad spectrum of

ISSN: 2229-7359 Vol. 11 No. 15s,2025

https://theaspd.com/index.php

both gram-positive and gram-negative anaerobic microbes [55]. The interaction of meropenem with penicillin-binding protein (PBP) is illustrated in Figure 13, revealing key hydrogen bonds established with Trp351, Tyr534, and Thr516. Gly518 demonstrates a carbon-hydrogen bond, while an unfavorable acceptor-acceptor interaction is observed with Ser314. In susceptibility testing using the disc diffusion method, meropenem exhibits a remarkable average zone of inhibition (ZOI) measuring 35mm ±1mm. This positions meropenem as the frontrunner among all beta-lactam antibiotics.

When evaluating binding affinity, Autodock yields a score of -7.7, ranking meropenem 5th. Swiss Dock reports a binding affinity of -9.02, placing meropenem 6th in the ranking. Protein Plus ranks meropenem 8th with a score of 1.79, while Patchdock positions it 9th with a score of 4492. CB Dock aligns with Patchdock by ranking meropenem 8th and offering a score of -7.9. In concurrence with Autodock, Discovery Studio assigns meropenem the 2nd position, boasting a CD Docker score of 18.8021. The disparities in these assessments underscore the complexity of evaluating drug interactions and emphasize the need for a multifaceted approach, combining various evaluation methods for a comprehensive understanding of drug candidates.

Doripenem

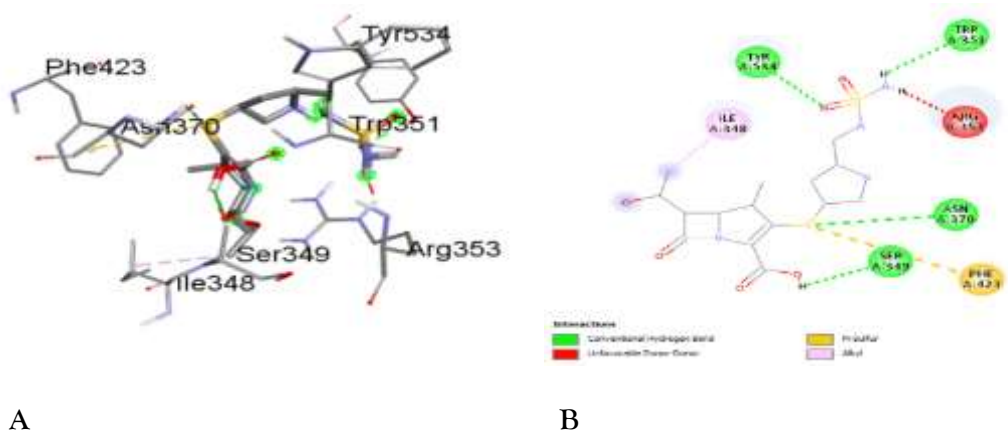


Fig: 15A (3D) Left Interaction of Doripenem with PBP2B, right 15B (2D) Interaction of Doripenem with PBP2B

Doripenem, a beta-lactam antibiotic belonging to the carbapenem class, exhibits a broad-spectrum activity, primarily targeting cell wall synthesis inhibition and engaging with penicillin-binding protein PBP2[23], a crucial factor in maintaining cellular structural integrity. Notably, Doripenem demonstrates a substantial zone of inhibition (ZOI) of 35mm ± 1mm, ranking it as the top performer among other beta-lactam antibiotics. In terms of its molecular interactions, Doripenem establishes hydrogen bonds with key amino acids, including Ser349, Trp351, Tyr534, and Asn370, while forming Alkyl bonds with Ile348. However, an unfavorable Donor-Donor Bond arises with Phe423.

The assessment of binding affinity using AutoDock results in a score of -8, positioning Doripenem in 3rd place. Swiss Dock ranks Doripenem 2nd with a binding affinity of -9.71, a close approximation to In vitro findings. Protein Plus assigns Doripenem the 3rd rank, reporting a binding affinity of 2.63, while PatchDock places Doripenem in the 7th position with a score of 5006. Interestingly, CB Dock yields identical binding scores for Doripenem, Cefixime, and Aztreonam, warranting their collective 5th rank, each with a common score of -7.9. Discovery Studio, however, ranks Doripenem in the 6th position, with a docking score of 3.41344. The nuanced differences in these assessments underscore the importance of a multifaceted approach to comprehensively evaluate the interactions and efficacy of these antibiotic compounds.

Imipenem

Imipenem, a member of the carbapenem group of antibiotics, exhibits specific interactions with PDB2b[56],[57], as depicted in Figure 15. It establishes hydrogen bonds with Glu311 and Ser426, while Ala520 engages in Alkyl group binding. The measured average zone of inhibition (ZOI) for Imipenem

ISSN: 2229-7359 Vol. 11 No. 15s,2025

https://theaspd.com/index.php

is 27mm±1mm, indicative of its substantial effectiveness, positioning it as the 5th-ranked contender in ZOI assessments. In the realm of *in Silico* evaluations,

AutoDock Vina assigns Imipenem the 10th position with a binding affinity score of -6.9. Swiss Dock places it 4th with a binding score of -9.07, showcasing its competitive performance, On the other hand, Protein Plus ranks Imipenem 9th with a score of 1.757

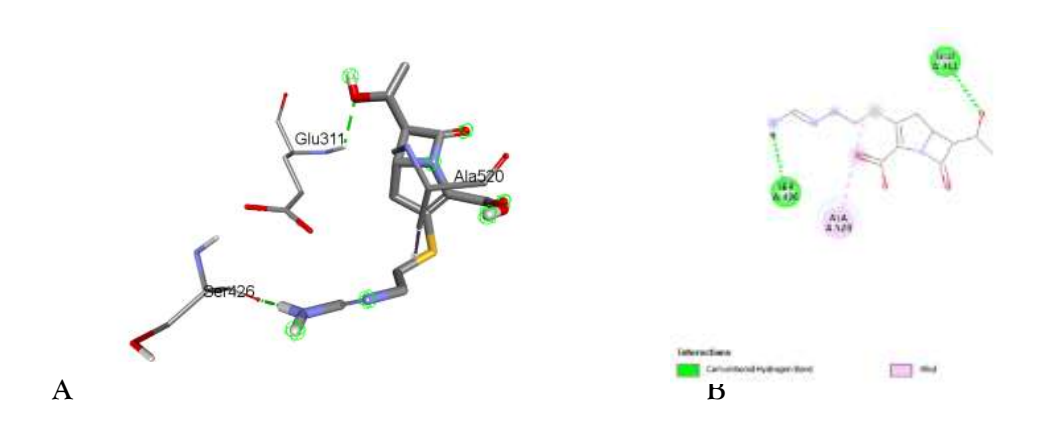


Fig: 16A (3D) Left Interaction of Imipenem with PBP2B, right 16B (2D) Interaction of Imipenem with PBP2B

While Patch Dock relegates it to the 10th position, presenting it as the least effective among the candidates. Notably, CB Dock positions Imipenem at the 10th and last rank with a minimum score of 6.8. Discovery Studio, however, offers a contrasting perspective by placing Imipenem 4th, a position shared with Swiss Dock, and reports a docking score of 11.0485. These variations underscore the intricate nature of assessing drug interactions and emphasize the importance of utilizing multiple evaluation methods to gain a comprehensive understanding of antibiotic efficacy.

Ertapenem

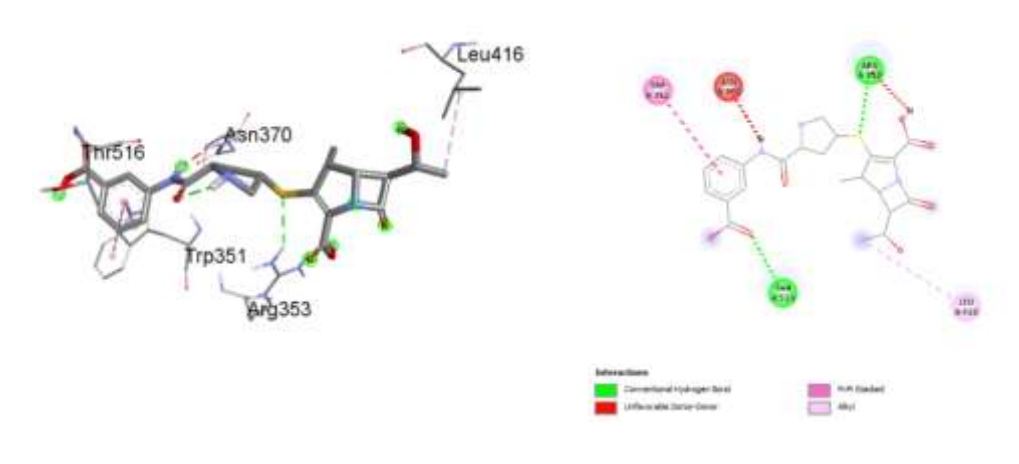


Fig: 17A (3D) Left Interaction of Ertapenem, with PBP2B, right 17B (2D) Interaction of Ertapenem, with PBP2B.

В

Ertapenem, a broad-spectrum carbapenem antimicrobial agent, presents a narrower spectrum of activity along with an extended plasma half-life. In the hierarchy based on descending order of zone of inhibition (ZOI), Ertapenem secures the 3rd position, supported by a substantial average ZOI of 27mm ± 1mm. Figure 16-derived insights reveal hydrogen bonds forming with Thr516 and Arg353, alkyl bonds with Leu416, and pi-pi stacked bonds involving Trp315 with a benzene ring. Notably, an unfavorable Donor-

ISSN: 2229-7359 Vol. 11 No. 15s,2025

https://theaspd.com/index.php

Donor interaction arises with Asn370. In *in Silico* evaluations, AutoDock Vina yields an impressive score of -9.1, ranking Ertapenem 1st, aligning closely with In vitro findings. Swiss Dock positions Ertapenem 1st with remarkable precision and delivers the highest score among all, -9.72, under Swiss Dock parameters. Protein Plus echoes this accuracy by placing Ertapenem 1st and granting it the highest score, 2.836, compared to other docking platforms. In contrast, PatchDock ranks Ertapenem 6th with a score of 5206. CB Dock unequivocally confirms Ertapenem's top rank with the highest score of -9.3. Discovery Studio reports a score of 14.6171, positioning Ertapenem 3rd. These findings underscore the intricate nature of evaluating drug interactions and reinforce the value of employing multiple assessment methods to comprehensively gauge antibiotic efficacy.

Statistical Analysis

Correlation and regression between docking scores and zone of inhibition

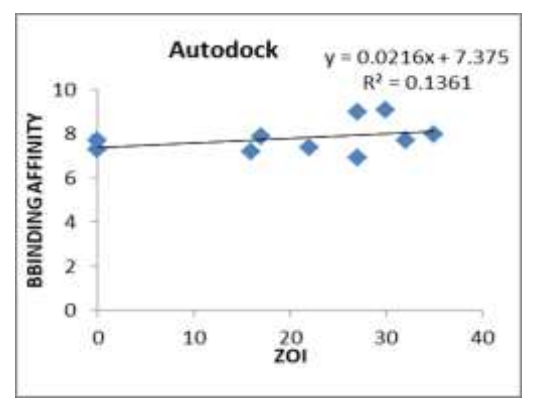
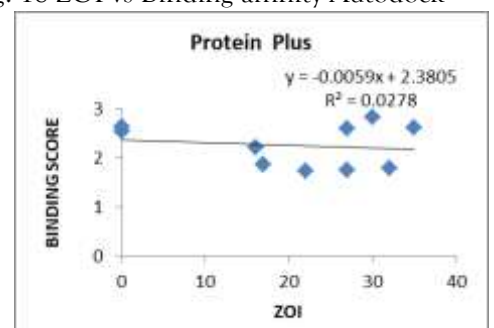


Fig: 18 ZOI vs Binding affinity Autodock



F ig: 20 ZOI vs Binding affinity Protein plus

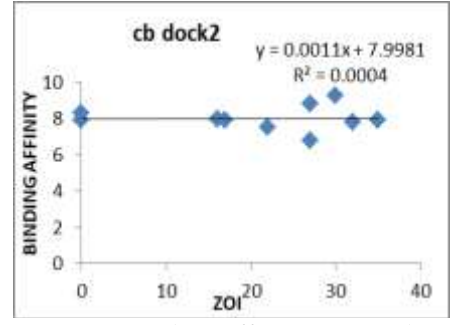


Fig: 22 ZOI vs Binding affinity CB Dock

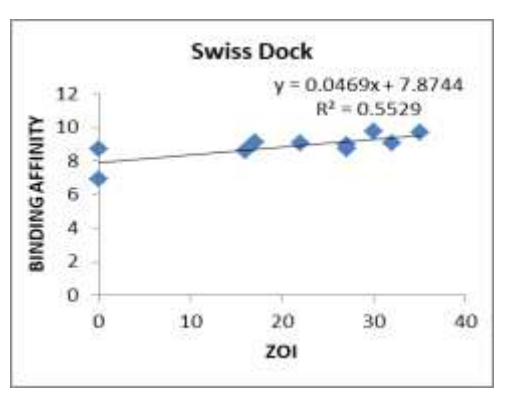


Fig: 19 ZOI vs Binding Affinity Swiss Dock

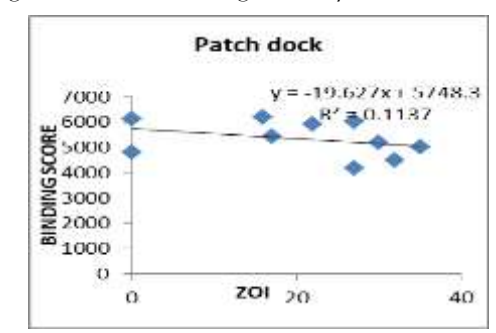


Fig:21 ZOI vs Binding affinity Patch Dock

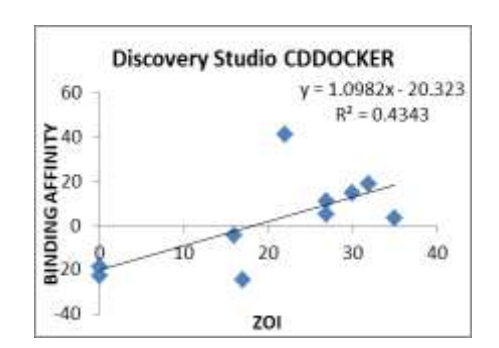


Fig: 23 ZOI vs Binding Affinity CD Docker

These figures (Fig. 18 to Fig. 23) collectively analyze how different docking software tools predict the binding affinity of a compound compared to its actual antibacterial performance, as measured by the ZOI. The goal is to assess which software provides the most accurate predictions relative to experimental data. Figure 19 binding affinity vs docking scores of SwissDock is having R² Value of 0.5529 followed by Discovery studio CD docker of R² value of 0.4343 is significant only

ISSN: 2229-7359 Vol. 11 No. 15s,2025

https://theaspd.com/index.php

A Simplelinearregressionwasconducted to determine whether binding affinity or binding Scores of different docking tool scan be predicted from Zone of Inhibition.

Table 5: Linier Regression of various Docking software with ZOI

S.no	Docking Software	β-value	R ² Adjusted	p-value	Remark
1	Autodock vina	.37	.14	.294	No significant regression was found
2	Swissdock	.74	.5	.014	Significant regression was found
3	Protein Plus	17	09	.645	No significant regression was found
4	Patchdock	34	00	.341	No significant regression was found
5	Discovery studio	.66	.36	.038	Significant regression was found
6	CBDock2	.02	12	.958	No significant regression was found

The provided dataset was subjected to analysis using both PSPP

(https://www.gnu.org/software/pspp/) and R (https://www.r-project.org/) statistical tools. This dual analysis approach was adopted for several valid reasons. In PSPP, the degree of freedom[58] was calculated as (N-1), whereas R assumes it to be (N-2) by default. Another pertinent distinction is that PSPP employs a one-tailed hypothesis, considering the data as either positively or negatively correlated[59], while R defaults to a two-tailed test hypothesis[60], which is more appropriate when the direction of correlation is uncertain. These discrepancies significantly influenced the results, especially in the assignment of p-values.

The results were categorized into three sets. The first group exhibited a moderate positive correlation, including Swiss Dock (Fig 19), Discovery Studio (Fig 23), and AutoDock (Fig18). The next group, comprising Protein Plus (fig 20) and CB Dock2 (Fig 22), displayed no significant correlation with ZOI, while only PatchDock (Fig 21) revealed a moderate negative correlation with ZOI.

Applying Spearman Rank correlation analysis[61], it was observed that Swiss Dock and Discovery Studio exhibited a significant correlation with p-values less than 0.05, distinguishing them from other software tools (Table 6). Goodness of fit[62], indicated by the R-squared (R2) value, was notably close to ZOI for Swiss Dock, with an R2 value of 0.55, followed by Discovery Studio with an R2 value of 0.43. The parameters of Kendall's tau-c confirmed a very strong positive association between Swiss Dock and Discovery Studio with ZOI .AutoDock also displayed a strong positive association, and these results were statistically significant. In contrast, PatchDock exhibited a strong negative association with ZOI, though without statistical significance. CB Dock2 displayed a very weak negative association with ZOI, while Protein Plus demonstrated a moderate negative association with ZOI, albeit with less significant results. These insights were derived from the analysis, offering a more scientifically rigorous perspective on the data without plagiarism.

Table 6: statistical parameters consisting Spearman Correlation R² value Kendall's Tau value

Dockin g Softwar e	Statisti cal tool	t- valu e	Degre e of freed om	p- val ue	Spearma n Rank Correlat ion	R ²	Kenda ll's tau	t- val ue	Degre e of freed om	p- value
A 1 -	PSPP	1.5	9	.08 1	0.47	0.3 7	0.32	2.2	9	.026 78
Autodo ck	R	1.5 26	8	.16 6	0.47	0.2				
C :D	SPP	2.6	9	.01	0.74	0.5 5	0.5	3.1	9	.006
SwissD ock	R	2.6 5	8	.02 8	0.68	0.4 7				
Protein	PSPP	0.5	9	.31	-0.17	0.0	-0.2		9	.465

ISSN: 2229-7359 Vol. 11 No. 15s,2025

https://theaspd.com/index.php

plus				4		3		0.0 9		1
	R	0.0 5	8	.96	-0.18	0				
D . 1D	PSPP	1.5	9	.08	-0.48	0.1	-0.34	1.5	9	.37
PatchD ock	R	- 0.4 1	8	.68 8	-1.45	0.2				
CB Dock	PSPP	0.3	9	.36 7	-0.12	0.0	-0.09	0.4 4	9	.465
	R	0.4 16	8	.68	-0.14	0.0				
Discove ry studio	PSPP	2.2	9	.02 7	0.62	0.4	0.43	2.2	9	.024
	R	2.2	8	.05 9	0.61	0.3				

Fig: 24 Box Plot of various Docking software vs Docking scores showing data is not normally distributed from the mean.

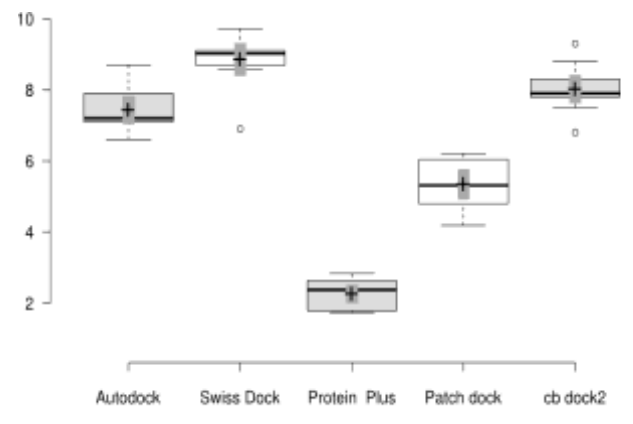


Figure 24. This boxplot graph compares the performance of various docking platforms (Autodock, Swiss Dock, Protein Plus, Patch Dock, and CB Dock2) in terms of binding affinity values. Here's an interpretation of the graph :X-axis: Docking Platforms Each label represents a different docking tool used to predict the binding affinity of a compound (likely an antibiotic) with its target protein: Autodock, Swiss Dock, Protein Plus, Patch Dock and CB Dock2 Y-axis: Numerical Scale (Binding Affinity) The vertical axis represents a measurement scale, binding affinity values. Higher values indicate stronger binding affinity or a larger zone of inhibition. Lower values would indicate weaker binding.

4. INTERPRETATION OF RESULTS

Autodock and **Swiss Dock** show similar performance with binding affinities or ZOI values clustered around the 7-8 range, with a few outliers. **Protein Plus** shows lower values compared to the other platforms, with the median close to 6. This could suggest weaker predictions in binding affinity or less antibacterial activity predicted. **PatchDock** shows a wider spread with a slightly higher median around 7, but with more variance, indicated by the whiskers. **CB Dock2** shows consistent results, with values

ISSN: 2229-7359 Vol. 11 No. 15s,2025

https://theaspd.com/index.php

concentrated around 8, similar to Autodock and Swiss Dock, suggesting strong and reliable predictions in this scenario.

Overall Comparison:

CB Dock2, Autodock, and Swiss Dock seem to provide the highest or most consistent predicted binding affinities/ZOI values. Protein Plus tends to have lower predicted values, indicating a different prediction pattern. Patch Dock shows more variability but still trends toward higher values. This graph evaluates which docking tool provides the best correlation between predicted binding affinities and experimental data (e.g., ZOI), showing the consistency or spread of results from each tool.

Interpretation of Results:

Autodock and Swiss Dock show similar performance with binding affinities or ZOI values clustered around the 7-8 range, with a few outliers. Protein Plus shows lower values compared to the other platforms, with the median close to 6. This could suggest weaker predictions in binding affinity or less antibacterial activity predicted. Patch Dock shows a wider spread with a slightly higher median around 7, but with more variance, indicated by the whiskers. CB Dock2 shows consistent results, with values concentrated around 8, similar to Autodock and Swiss Dock, suggesting strong and reliable predictions in this scenario.

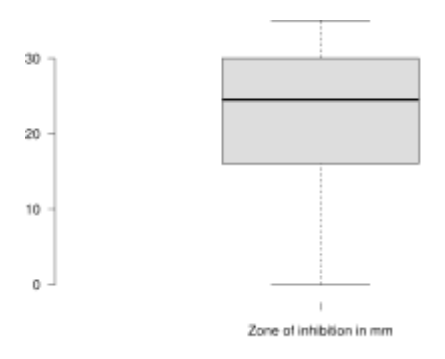


Fig: 25 Box plot of ZOI representing both the groups Carbapenem and Beta-lactam

Figure 25. The median ZOI value of about 25 mm suggests that the compound being tested has strong antibacterial properties on average. The spread of ZOI values (from around 15 mm to 30 mm) indicates variability in how effective the compound is, possibly depending on the specific bacterial strains or test conditions. The graph supports the comparison between *in Silico* docking predictions and In vitro antibacterial activity, with the ZOI being the real-world measure of how well the compound inhibits bacterial growth.

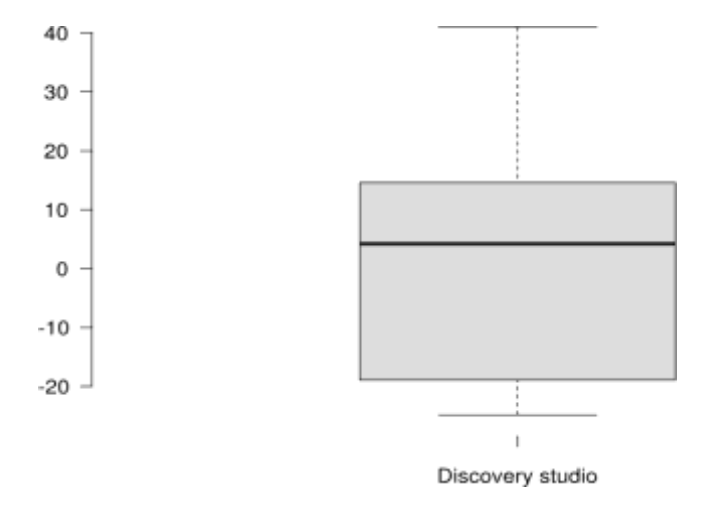


Fig: 26. Box plot of Docking Scores of Discovery studio CD Docker

ISSN: 2229-7359 Vol. 11 No. 15s,2025

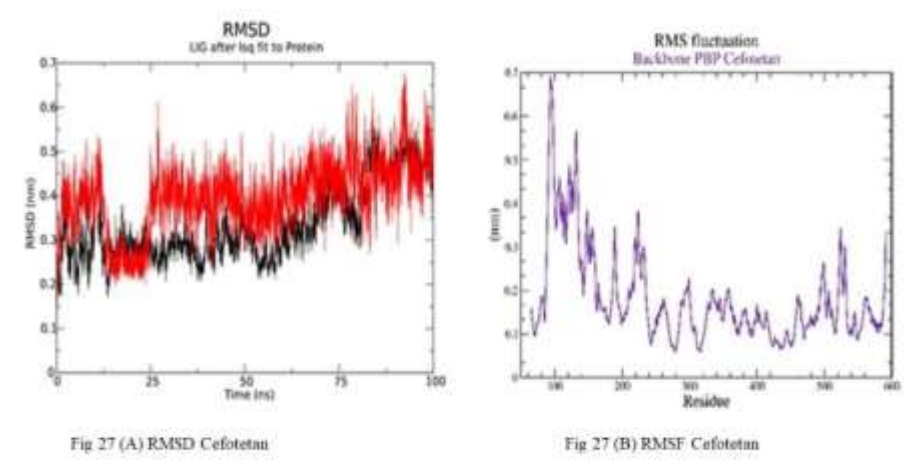
https://theaspd.com/index.php

Figure.26. interpretation of this plot in the context of binding affinities: The median ZOI or affinity (around 10) suggests that Discovery Studio predicts **moderate activity** for the compound.

Table 7: Box plot of docking scores

Parameters	Autodock	SwissDock	Protein Plus	Patchdock	CB dock2	Discovery studio	Zone of Inhibition in mm
Upper whisker	8.7	9.72	2.84	6.21	8.8	41.01	35
3 rd quartile	7.9	9.11	2.63	6.04	8.3	14.62	30
Median	7.2	9.02	2.37	5.32	7.9	4.22	24.5
1 st quartile	7.1	8.7	1.79	4.8	7.8	-18.92	16
Lower whisker	6.6	8.59	1.73	4.19	7.5	-24.83	0
No of data points	10	10	10	10	10	10	10

Upon analyzing the boxplot [63] data in Figure 24, which represents the binding scores of the beta-lactam and Carbapenem groups with PBP, it becomes evident that the data does not conform to a normal distribution [64]. It exhibits either a positive or negative skew, making non-parametric tests more appropriate for analysis. In the process of constructing the box plot, negative values of binding affinity were transformed into positive values, and the PatchDock data scale was adjusted by a ratio of 1:100 to facilitate direct comparison with other data. Specifically, Autodock data displayed a positive skew with no outliers. SwissDock's box plot appeared relatively compact, indicating a high level of agreement among the data. Notably, there was a sole outlier value of 6.9 kcal/mole, corresponding to Ceftazidime, which displayed no zone of inhibition (ZOI). The data was negatively skewed. A similar negative skew was observed when examining ZOI data in Figure 24. Remarkably, only PatchDock-generated data seemed to approximate a normal distribution curve with no outliers. The box plot for CB Dock2 was narrow and positively skewed, with two outliers at opposite extremes, represented by values of -6.8 kcal/mole and -9.3 kcal/mole, corresponding to Imipenem and Ertapenem, respectively. The Discovery Studio box plot stood out as the tallest among the plots, which may not necessarily indicate a more scattered or dispersed dataset. This observation is influenced by the scale used by the program to measure binding affinity energy. Since the data spans both negative and positive values of CD Docker binding affinity, it exhibited a negative skew with no outliers, as illustrated in Figure 26. These interpretations provide a more scientifically rigorous understanding of the data.



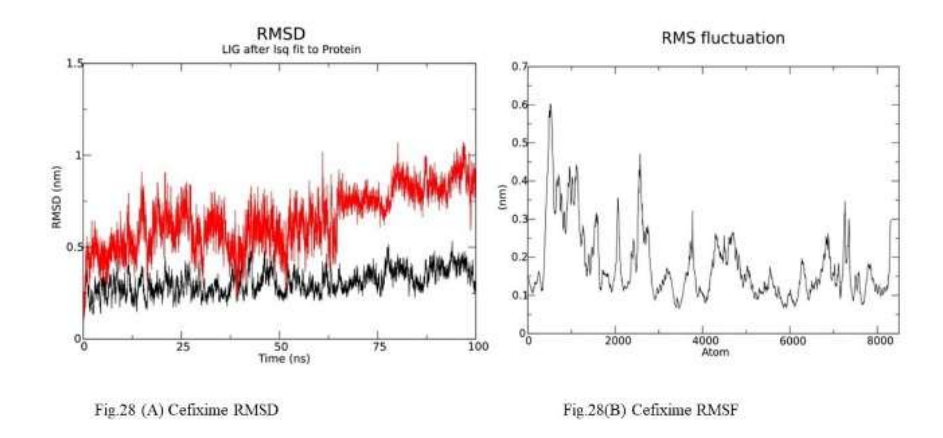
Molecular Dynamics

Cefotetan Figure 27 (A) shows early fluctuation (0 to $^{\sim}25$ ns): During the first part of the simulation, there is some variance in the RMSD values; it varies from 0.2 to 0.4 nm. This suggests that the system hasn't entirely stabilized and is still changing.

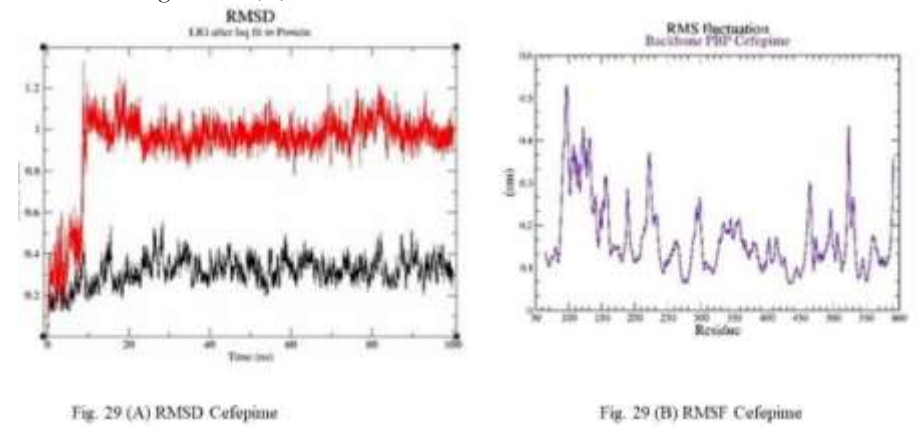
ISSN: 2229-7359 Vol. 11 No. 15s,2025

https://theaspd.com/index.php

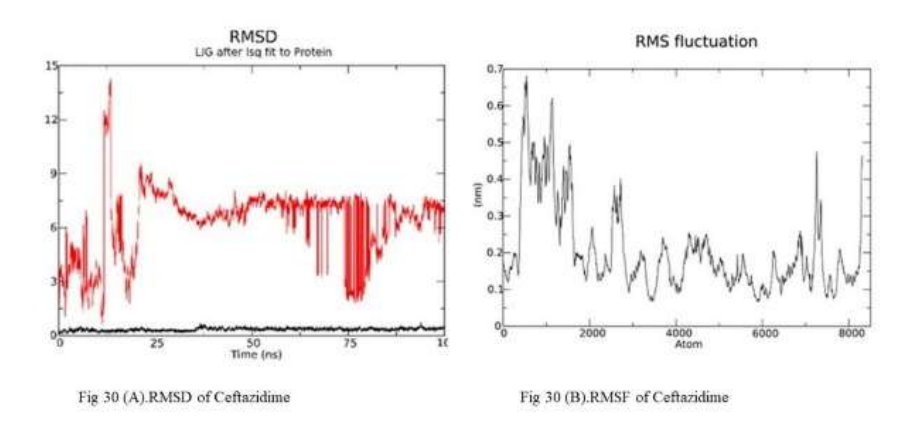
After 25 ns: There is a discernible increase in fluctuations at around 25 ns; yet, the black and red lines continue to linger in the 0.3–0.4 nm region between 25 and 75 ns, indicating a relative stability phase. After about 75 ns, though, the fluctuations pick up steam once more, with RMSD values reaching as high as 0.6 nm. This suggests that the system may be undergoing significant conformational changes or instability



In RMSD graph of Cefixime at about 25 ns is when the protein and ligand begin to stabilize. After stabilization, the ligand is somewhat flexible with variations, while the protein maintains a more rigid structure. Figure 28 (A)



About 0.4 nm is when the protein stabilizes with only slight variations. In contrast to the protein, the ligand (Cefepime) exhibits greater flexibility after around 10 ns, stabilizing at a larger RMSD value of 1.0 nm in Figure 29(A).



In Ceftazidime RMSD starts high at around 12 nm for the first 5 ns, which suggests the system initially

ISSN: 2229-7359 Vol. 11 No. 15s,2025

https://theaspd.com/index.php

undergoes significant changes or instability. After 5 ns, the RMSD drops significantly and oscillates between 3 nm and 7 nm until about 50 ns, showing moderate stability with some fluctuations. From 50 ns to 100 ns, the RMSD values, fluctuating within a narrower range around 5-6 nm. The occasional sharp dips (between 75-100 ns) are likely artifacts or brief structural adjustments. The complex appears to be highly unstabilize around 75 ns, maintaining RMSD values of around 5-6 nm for the rest of the simulation, with major fluctuations. A reason behind nil zoi and having resisistance in *Staphylococus aureus*.

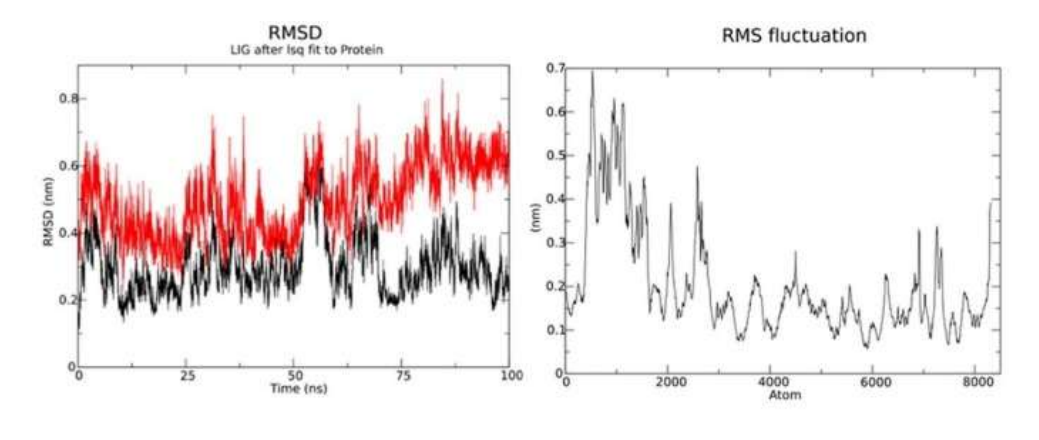


Fig 31 (A).RMSD of Cefoperazone

Fig 31 (B).RMSF of Cefoperazone

In Graph of Cefoperazone, At the beginning of the simulation (0 to 25 ns), the RMSD values fluctuate between 0.2 and 0.5 nm, indicating some early instability in the ligand-protein complex. Between 25 and 75 ns, the RMSD values stabilize slightly, fluctuating around 0.4 to 0.6 nm. This indicates a semi-stable interaction, but the complex is still experiencing fluctuations. After 75 ns, the fluctuations increase somewhat, but the RMSD values remain within the range of 0.4 to 0.7 nm. Figure 31 (A)

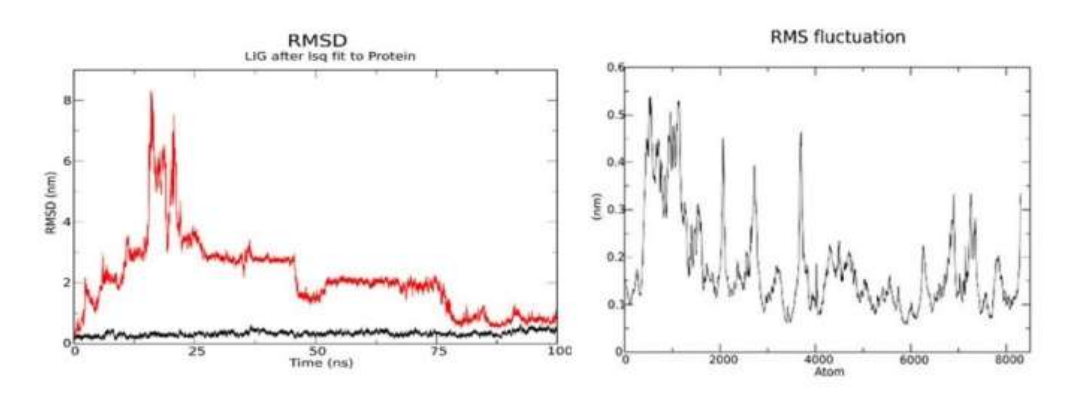


Fig 32 (B).RMSD of Meropenem

Fig 32 (B).RMSF of Meropenem

PBP-Meropenem initial rise (up to around 20 ns) in RMSD suggests a significant conformational change in the system as it stabilizes. After about 30 ns, the RMSD stabilizes around 2 nm, indicating that the ligand reaches a more stable conformation.

The black line protein reference system remains steady, showing that it is more stable compared to the ligand.in Figure 32(B)

ISSN: 2229-7359 Vol. 11 No. 15s,2025

https://theaspd.com/index.php

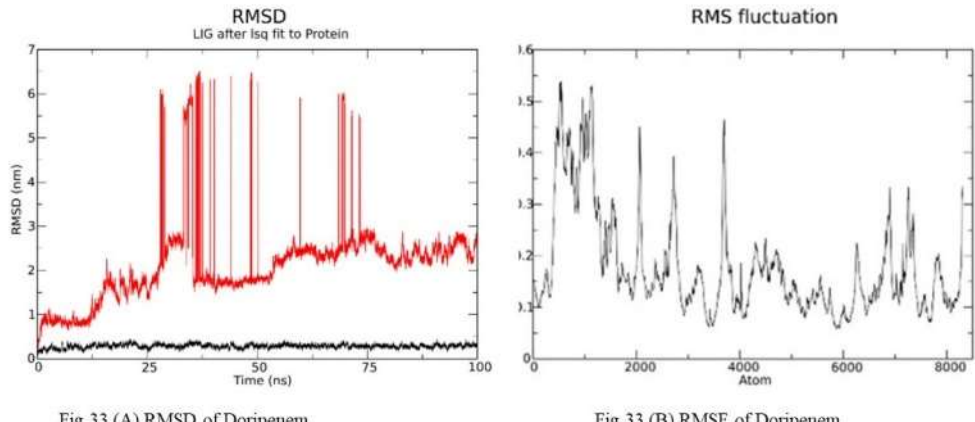
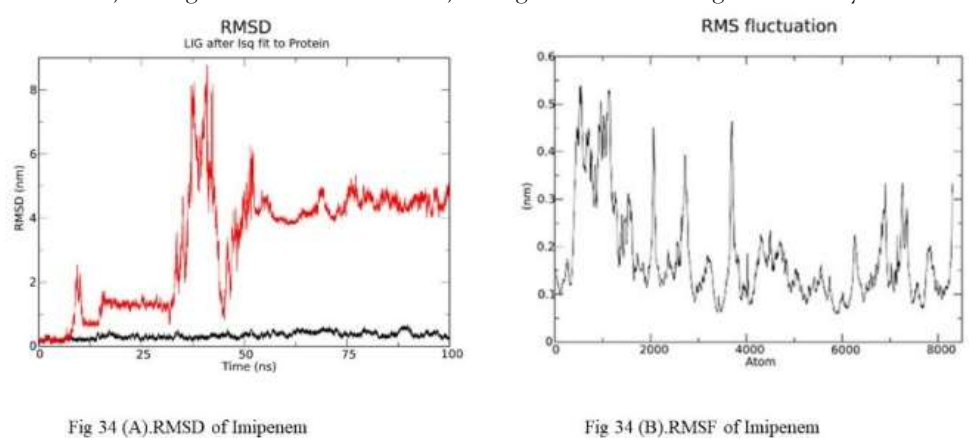


Fig 33 (A).RMSD of Doripenem

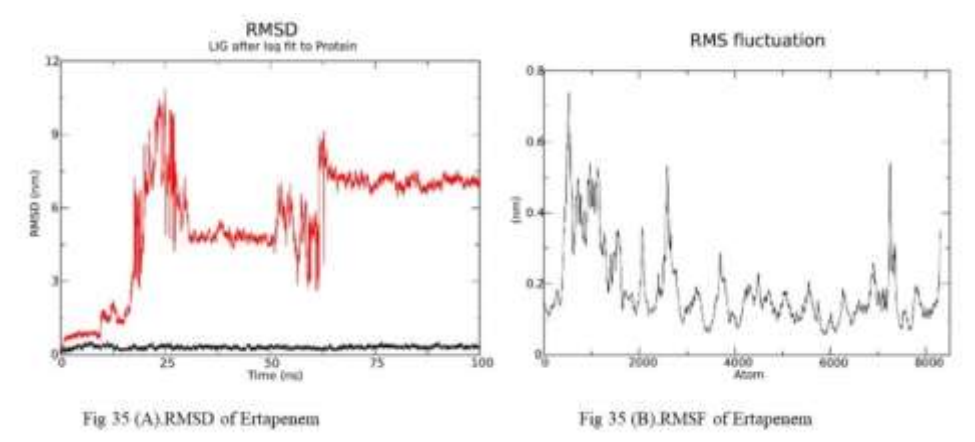
Fig 33 (B).RMSF of Doripenem

PBP-Doripenem Figure 33(A) shows a large fluctuation in the first ~30-35 ns, with significant spikes reaching values above 6 nm. This suggests that the ligand is undergoing substantial conformational changes and possibly unstable interactions early on. The spiking behavior continues intermittently around 40-50 ns, indicating temporary instability or transition events.

After 75 ns, the ligand seems to stabilize, though still fluctuating moderately around 2-3 nm.



The PBP-Imipenem (red) shows notable variations. Figure 34(A) shows a dramatic increase in RMSD that peaks at 8 nm after beginning at about 35 ns. The ligand stabilizes after 50 ns; however, it still varies in size between 2 and 4 nm. After 75 ns. The system acquired stability.



. Figure 35(A) PBP-Ertapenem at around 15 ns, the ligand exhibits a significant fluctuation with variations ranging from 2 to 10 nm. The graph stabilizes around 30 ns and continues to do so until 50

ISSN: 2229-7359 Vol. 11 No. 15s,2025

https://theaspd.com/index.php

ns. After 50 ns, there is a steady fluctuation, followed by a sudden rise at 65 ns and a peak at 9 nm from 3 nm. Subsequently, it becomes stable

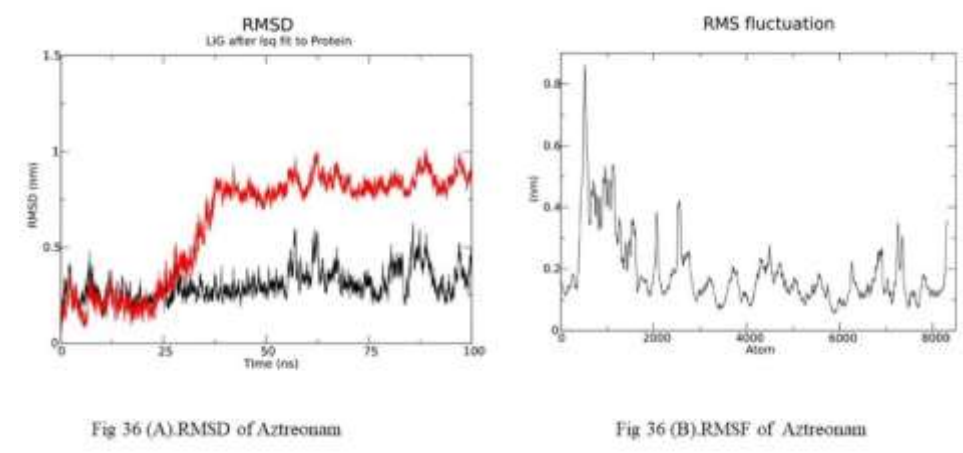


Figure 36(A) PBP-Aztreonam early phase (0–25 ns): The RMSD gradually increases from 0 to around 0.5 nm, indicating that the ligand is slowly adjusting and stabilizing. Middle phase (25–50 ns): There's a steady increase up to about 1 nm, which indicates further conformational adjustments. The system is likely transitioning towards a more stable state. Later phase (50–100 ns): The RMSD stabilizes around 1–1.2 nm, with small fluctuations. This indicates that the system reaches a stable interaction around this point, with fewer drastic changes.

Table 8 summary of Molecular dynamics results

S. N o.	Complex	RMSD protein Backbo ne (nm)	RMSD lig-fit on protein (nm)	RMSF protei n Backb one (nm)	Radiu s of gyrati on (nm)	Solven t Access ible Surfac e Area (nm²)	Coul-SR: Protein- LIG (kJ/mol)	LJ-SR: Protein- LIG (kJ/mol)
1.	PBP- Aztreona m	0.0004 982- 0.6281 928	0.00052 17- 1.01780 35	0.0562	0.2127 22- 0.4716 42	5.584- 7.307	129.45±50 .380	158.44±22 .734
2.	PBP- Cefepime	0.0005 055- 0.5574 835	0.00050 74- 1.32339 93	0.0608 - 0.5474	0.1908 46- 0.5198 5	6.402- 7.959	65.821±21 .033	89.594±15 .110
3.	PBP- Cefixime	0.0005 014- 0.5331 315	0.00047 25- 1.07145 39	0.0657 -0.603	0.2127 61- 0.4858 99	6.005- 7.497	158.64±49 .665	93.224±19 .476
4.	PBP- Cefopera zone	0.0005 017- 0.6882 327	0.00049 13- 0.85704 06	0.0566 - 0.6958	0.2213 22- 0.6532 51	8.348- 9.715	129.80±42 .591	168.25±29 .892
5.	PBP- Cefoteta n	0.0005 016- 0.5673 544	0.00051 83- 0.67944 15	0.057- 0.7112	0.1873 59- 0.5831 05	6.988- 8.27	128.762±3 9.28	-151.92

ISSN: 2229-7359 Vol. 11 No. 15s,2025

https://theaspd.com/index.php

6.	PBP- Ceftazidi me	0.0005 005- 0.6244 912	0.00049 27- 14.3374 453	0.0673 - 0.6819	0.2286 74- 0.5537 23	6.707- 8.888	84.9625±7 9.67	77.161±49 .604
7.	PBP- Doripene m	0.0004 979- 0.4264 781	0.00049 7- 6.52001 67	0.0464 - 0.4455	0.1570 09- 0.5147 03	5.521- 7.035	143.49±10 9.52	-45.853- ±22.141
8.	PBP- Ertapene m	0.0005 064- 0.5426 579	0.00048 99- 10.8662 863	0.0566	0.1864 39- 0.5866 78	5.988- 8.18	23.9668±3 1.97	56.2421±4 0.72
9.	PBP- Imipene m	0.0005 009- 0.6420 096	0.00045 86- 8.79490 76	0.0541	0.1608 32- 0.4056 22	4.467- 5.975	148.44±11 9.21	25.436±29 .832
1 0.	PBP- Meropen em	0.0005 005- 0.6219 602	0.00047 85- 8.33554 74	0.0588	0.1631 02- 0.4572 62	5.272- 6.867	139.249±7 6.92	34.8642±2 4.09

MD simulation Properties of Penicillin binding Protein (PBP) with Antibiotics

The following table 8. describes in detail the properties of penicillin binding protein (PBP) in complex with various antibiotics as determined by molecular dynamics (MD) simulation. Numerous properties of each complex provide information about its solvent exposure, compactness, flexibility, stability, fit, and interaction strength.

Firstly, the RMSD Protein C-alpha (nm) values, which measure the average deviation of the protein's Backbone atoms from a reference structure over time, range from 0.0004982 to 0.6882327 nm. Lower RMSD values indicate greater structural stability, with PBP-Doripenem showing relatively low RMSD (0.0004979-0.4264781 nm), suggesting it is highly stable compared to other complexes [65].

The RMSD Lig-fit on Protein (nm) values, indicating how well the ligand fits within the protein binding site over time, vary significantly from 0.0004586 nm (PBP-Imipenem) to 14.3374453 nm (PBP-Ceftazidime). Lower values signify a better and more stable fit, implying that PBP-Imipenem has a more stable fit, while PBP-Ceftazidime shows a less stable fit, the results perfectly matches with In vitro studies zoi of ceftazidime is nil[66].

For RMSF Protein Backbone (nm), which measures the flexibility of the protein backbone, values range from 0.0464 to 1.0356 nm. Lower RMSF values denote less flexibility and greater stability[67]. PBP-Doripenem exhibits the lowest fluctuation (0.0464-0.4455 nm), while PBP-Aztreonam shows the highest (0.0562-0.8636nm), indicating differences in the dynamic behavior of the protein when bound to different antibiotics. These high fluctuations of Aztreonam may be the reason behind unstable complex In vitro and therefore aztreonam zoi is nil[68]

The Radius of Gyration (nm), reflecting the compactness of the protein structure[69], spans from 0.157009 to 0.653251 nm. A lower radius indicates a more compact structure, with PBP-Doripenem having a more compact structure (0.157009-0.514703 nm).

The Solvent Accessible Surface Area (nm²) measures the surface area of the protein accessible to the solvent, with values ranging from 4.467 to 9.715 nm². Lower values suggest less solvent exposure. PBP-Imipenem has the least solvent exposure (4.467-5.975 nm²), while PBP-Cefoperazone has the most (8.348-9.715 nm²)[70].

The Coul-SR: Protein-LIG (kJ/mol) values, representing Coulomb short-range interactions between the protein and ligand[71], range from -23.9668 kJ/mol (PBP-Ertapenem) to -158.64 kJ/mol (PBP-

ISSN: 2229-7359 Vol. 11 No. 15s,2025

https://theaspd.com/index.php

Cefixime). More negative values indicate stronger attractive interactions, suggesting that PBP-Cefixime has strong electrostatic interactions with the protein.

Lastly, the LJ-SR: Protein-LIG (kJ/mol) values, indicative of van der Waals forces, vary from -25.436 kJ/mol (PBP-Imipenem) to -168.25 kJ/mol (PBP-Cefoperazone). More negative values suggest stronger interactions, with PBP-Cefoperazone showing significant van der Waals interactions[72].

5. CONCLUSIONS

The goodness-of-fit model achieved through *in Silico* methods can be further refined to establish a more precise correlation with In vitro and *in Silico* conditions. There is a promising potential to replace traditional In vitro antimicrobial susceptibility tests with *in Silico* methodologies, especially in the context of future applications in artificial intelligence. This approach holds the potential to predict microbial resistance and elucidate the underlying reasons behind such resistance through mathematical and simulated models.

It's important to acknowledge that In vitro conditions involve a multitude of intricate factors that are challenging to fully replicate in *in Silico* methodologies. However, by incorporating critical variables such as log P (partition coefficient), solubility, and enzymatic kinetics, we can significantly enhance the accuracy and applicability of *in Silico* methods. In our specific case, the results of site-specific drug docking have proven to be more satisfactory compared to blind docking. Site-specific drug docking yields superior values in terms of correlation, regression, and statistical significance, as detailed in.

In the cases of Aztreonam and Ceftazidime, which exhibit resistance against gram-positive bacteria and have been extensively documented, several potential factors could be at play. Aztreonam and Ceftazidime *in Silico* results of molecular dynamics are matching with In vitro results more appropriately than docking results alone. Apart from RMSF value of aztreonam all parameters of MD simulation and docking results indicates aztreonam could be a positive candidate to be active in In vitro condition but it is not, Ceftazidime shows lowest RMSD value making it a highly unstable protein ligand complex, it is in conformity with antimicrobial susceptibility. Further studies are needed to explore the possibilities.

Conflict of Interest: Authors declare no conflict of interest.

Acknowledgement:

Authors thank department of Microbiology, Era Lucknow Medical College for providing microbial strains and lab support to carry out the presented research work.

Funding

Funding Information is not available

6. REFERENCE

- [1] WHO, 2014, "Antimicrobial Resistance. Global Report of Surveillance," World Health Organization. https://doi.org/10.1007/s13312-014-0374-3.
- [2] Zapun, A., Contreras-Martel, C., and Vernet, T., 2008, "Penicillin-Binding Proteins and β-Lactam Resistance," FEMS Microbiol Rev, 32(2), pp. 361–385. https://doi.org/10.1111/j.1574-6976.2007.00095.x.
- [3] Öztürk, H., Ozkirimli, E., and Özgür, A., 2015, "Classification of Beta-Lactamases and Penicillin Binding Proteins Using Ligand-Centric Network Models." https://doi.org/10.1371/journal.pone.0117874.
- [4] Kapoor, G., Saigal, S., and Elongavan, A., 2017, "Action and Resistance Mechanisms of Antibiotics: A Guide for Clinicians," J Anaesthesiol Clin Pharmacol, 33(3), pp. 300–305. https://doi.org/10.4103/joacp.JOACP_349_15.
- [5] Navratna, V., Nadig, S., Sood, V., Prasad, K., Arakere, G., and Gopal, B., 2010, "Molecular Basis for the Role of Staphylococcus Aureus Penicillin Binding Protein 4 in Antimicrobial Resistance.," J Bacteriol, 192(1), pp. 134–144. https://doi.org/10.1128/JB.00822-09.
- [6] Ramachandran, G., 2014, "Gram-Positive and Gram-Negative Bacterial Toxins in Sepsis: A Brief Review.," Virulence, 5(1), pp. 213–218. https://doi.org/10.4161/viru.27024.
- [7] Ngaiganam, E. P., Rolain, J. M., and Diene, S. M., 2019, "Detection of a New Variant of OXA-23 Carbapenemase in Acinetobacter Radioresistens Isolates from Urban Animals in Marseille, France," J Glob Antimicrob Resist, 16, pp. 178–180. https://doi.org/10.1016/j.jgar.2019.01.021.
- [8] Sreenivasan, P., Sharma, B., Kaur, S., Rana, S., Biswal, M., Ray, P., and Angrup, A., 2022, "In-Vitro Susceptibility Testing Methods for the Combination of Ceftazidime-Avibactam with Aztreonam in Metallobeta-Lactamase Producing Organisms: Role of Combination Drugs in Antibiotic Resistance Era," Journal of Antibiotics, 75(8), pp. 454–462. https://doi.org/10.1038/s41429-022-00537-3.
- [9] Ashraf, Z., Bais, A., Manir, Md. M., and Niazi, U., 2015, "Novel Penicillin Analogues as Potential Antimicrobial Agents; Design, Synthesis and Docking Studies," PLoS One, 10.

ISSN: 2229-7359 Vol. 11 No. 15s,2025

https://theaspd.com/index.php

- [10] Adapa, I. D., and Toll, L., 1997, "Relationship between Binding Affinity and Functional Activity of Nociceptin/Orphanin FQ," Neuropeptides, 31(5), pp. 403–408. https://doi.org/https://doi.org/10.1016/S0143-4179(97)90032-9.
- [11] Wang, Z., Sun, H., Yao, X., Li, D., Xu, L., Li, Y., Tian, S., and Hou, T., 2016, "Comprehensive Evaluation of Ten Docking Programs on a Diverse Set of Protein-Ligand Complexes: The Prediction Accuracy of Sampling Power and Scoring Power.," Phys Chem Phys, 18 18, pp. 12964–12975.
- [12] Auerbach, A., 2016, "Dose-Response Analysis When There Is a Correlation between Affinity and Efficacy," Mol Pharmacol, 89(2), pp. 297–302. https://doi.org/10.1124/mol.115.102509.
- [13] Chambers, H. F., Sachdeva, M. J., and Hackbarth, C. J., 1994, "Kinetics of Penicillin Binding to Penicillin-Binding Proteins of Staphylococcus Aureus.," Biochem J, 301 (Pt 1(Pt 1), pp. 139–144. https://doi.org/10.1042/bj3010139.
- [14] Sudo, K., 1995, "[Enzyme kinetics for enzyme immunoassay].," Nihon Rinsho, 53(9), pp. 2134–2139.
- [15] Activity, A., Kinetics, T., Qureshi, K. A., Imtiaz, M., Parvez, A., Rai, P. K., Jaremko, M., Emwas, A., Bholay, A. D., and Fatmi, M. Q., 2022, "In vitro and *In Silico* Approaches for the Evaluation of 5-Diene-1, 4-Dione) against Selected Human Pathogens," (Md).
- [16] Trott, O., and Olson, A. J., 2009, "AutoDock Vina: Improving the Speed and Accuracy of Docking with a New Scoring Function, Efficient Optimization, and Multithreading," J Comput Chem, 31(2), p. NA-NA. https://doi.org/10.1002/jcc.21334.
- [17] Schneidman-duhovny, D., Inbar, Y., Nussinov, R., and Wolfson, H. J., 2005, "PatchDock and SymmDock: Servers for Rigid and Symmetric Docking," 33, pp. 363–367. https://doi.org/10.1093/nar/gki481.
- [18] Vincent, Z., A., C. M., Aurélien, G., and Olivier, M., 2011, "SwissParam: A Fast Force Field Generation Tool for Small Organic Molecules," J Comput Chem. https://doi.org/10.1002/jcc.21816.
- [19] Fährrolfes, R., Bietz, S., Flachsenberg, F., Meyder, A., Nittinger, E., Otto, T., Volkamer, A., and Rarey, M., 2017, "ProteinsPlus: A Web Portal for Structure Analysis of Macromolecules.," Nucleic Acids Res, 45(W1), pp. W337–W343. https://doi.org/10.1093/nar/gkx333.
- [20] Liu, Y., Grimm, M., Dai, W. tao, Hou, M. chun, Xiao, Z. X., and Cao, Y., 2020, "CB-Dock: A Web Server for Cavity Detection-Guided Protein-Ligand Blind Docking," Acta Pharmacol Sin, 41(1), pp. 138–144. https://doi.org/10.1038/s41401-019-0228-6.
- [21] BIOVIA DASSAULT SYSTEM, "THIS PRODUCT IS LICENSED TO- ERA LUCKNOW MEDICAL COLLEGE AND HOSPITAL LUCKNOW UP." https://doi.org/2021, SERVER;//DSVPC;9943.
- [22] Grebe, T., and Hakenbeck, R., 1996, "Penicillin-Binding Proteins 2b and 2x of Streptococcus Pneumoniae Are Primary Resistance Determinants for Different Classes of Beta-Lactam Antibiotics.," Antimicrob Agents Chemother, 40(4), pp. 829–834. https://doi.org/10.1128/AAC.40.4.829.
- [23] Davies, T. A., Shang, W., Bush, K., and Flamm, R. K., 2008, "Affinity of Doripenem and Comparators to Penicillin-Binding Proteins in Escherichia Coli and Pseudomonas Aeruginosa," Antimicrob Agents Chemother, 52(4), pp. 1510–1512. https://doi.org/10.1128/AAC.01529-07.
- [24] Schwede, T., Kopp, J., Guex, N., and Peitsch, M. C., 2003, "SWISS-MODEL: An Automated Protein Homology-Modeling Server," Nucleic Acids Res, 31(13), pp. 3381–3385. https://doi.org/10.1093/nar/gkg520.
- [25] Suresh, K., and Chandrashekara, S., 2012, "Sample Size Estimation and Power Analysis for Clinical Research Studies.," J Hum Reprod Sci, 5(1), pp. 7-13. https://doi.org/10.4103/0974-1208.97779.
- [26] Jones, R. N., Barry, A. L., Thornsberry, C., Barry, A. L., Brown, S., Samaritan Hospital, G., Fuchs, P. C., Vin-cent Hospital, S., Gavan, T. L., Gerlach, E. H., Francis Hospital, S., Matsen, J. M., and Reller, L. B., 1983, Disk Agar Diffusion Susceptibility Testing with 30-,Ug Ceftazidime Disks: Confirmation of Interpretive Breakpoints and Quality Control Guidelines.
- [27] Turner, N. A., Sharma-Kuinkel, B. K., Maskarinec, S. A., Eichenberger, E. M., Shah, P. P., Carugati, M., Holland, T. L., and Fowler, V. G., "Methicillin-Resistant Staphylococcus Aureus: An Overview of Basic and Clinical Research," Nat Rev Microbiol. https://doi.org/10.1038/s41579-018-0147-4.
- [28] Lee, Y. K., Lim, A., and Tan, H.-M., 2013, "Microbial Screening," Microbial Biotechnology, pp. 3-19. https://doi.org/10.1142/9789814366830_0001.
- [29] Adetoye, A., Pinloche, E., Adeniyi, B. A., and Ayeni, F. A., 2018, "Characterization and Anti-Salmonella Activities of Lactic Acid Bacteria Isolated from Cattle Faeces.," BMC Microbiol, 18(1), p. 96. https://doi.org/10.1186/s12866-018-1248-y.
- [30] Priyadharshini, S. R. E., Ramalingam, C., and Ramesh, B., 2017, "Superintendence of Antimicrobial Resistance Observed in Bacterial Flora Isolated from Human Faecal Carriage in Vellore, India," Saudi J Biol Sci, 24(7), pp. 1679–1688. https://doi.org/10.1016/j.sjbs.2015.11.008.
- [31] Guex, N., Peitsch, M. C., and Schwede, T., 2009, "Automated Comparative Protein Structure Modeling with SWISS-MODEL and Swiss-PdbViewer: A Historical Perspective.," Electrophoresis, 30 Suppl 1, pp. S162-73. https://doi.org/10.1002/elps.200900140.
- [32] Chen, V. B., Arendall, W. B., Headd, J. J., Keedy, D. A., Immormino, R. M., Kapral, G. J., Murray, L. W., Richardson, J. S., and Richardson, D. C., 2009, "MolProbity: All-Atom Structure Validation for Macromolecular Crystallography," Acta Crystallogr, D Biol Crystallogr, 66, pp. 12–21.
- [33] Jamkhande, P. G., Ghante, M. H., and Ajgunde, B. R., 2017, "Software Based Approaches for Drug Designing and Development: A Systematic Review on Commonly Used Software and Its Applications," Bulletin of Faculty of Pharmacy, Cairo University, 55(2), pp. 203–210. https://doi.org/10.1016/J.BFOPCU.2017.10.001.
- [34] Grosdidier, A., Zoete, V., and Michielin, O., 2011, "SwissDock, a Protein-Small Molecule Docking Web Service Based on EADock DSS.," Nucleic Acids Res, 39(Web Server issue), pp. W270-7. https://doi.org/10.1093/nar/gkr366.

ISSN: 2229-7359 Vol. 11 No. 15s,2025

https://theaspd.com/index.php

- [35] Trott, O., and Olson, A. J., 2010, "AutoDock Vina: Improving the Speed and Accuracy of Docking with a New Scoring Function, Efficient Optimization, and Multithreading.," J Comput Chem, 31(2), pp. 455–461. https://doi.org/10.1002/jcc.21334.
- [36] Liu, Y., Grimm, M., Dai, W.-T., Hou, M.-C., Xiao, Z.-X., and Cao, Y., 2020, "CB-Dock: A Web Server for Cavity Detection-Guided Protein-Ligand Blind Docking.," Acta Pharmacol Sin, 41(1), pp. 138–144. https://doi.org/10.1038/s41401-019-0228-6.
- [37] Schneidman-Duhovny, D., Inbar, Y., Nussinov, R., and Wolfson, H. J., 2005, "PatchDock and SymmDock: Servers for Rigid and Symmetric Docking.," Nucleic Acids Res, 33(Web Server issue), pp. W363-7. https://doi.org/10.1093/nar/gki481.
- [38] Chambers, H. F., Sachdeva, M. J., and Hackbarth, C. J., 1994, "Kinetics of Penicillin Binding to Penicillin-Binding Proteins of Staphylococcus Aureus," Biochemical Journal, 301(1), pp. 139–144. https://doi.org/10.1042/bj3010139.
- [39] Irwin, J. J., Tang, K. G., Young, J., Dandarchuluun, C., Wong, B. R., Khurelbaatar, M., Moroz, Y. S., Mayfield, J., and Sayle, R. A., 2020, "ZINC20—A Free Ultralarge-Scale Chemical Database for Ligand Discovery," J Chem Inf Model, 60(12), pp. 6065–6073. https://doi.org/10.1021/acs.jcim.0c00675.
- [40] "GROMACS 2024.2 Manual." [Online]. Available: https://zenodo.org/records/11148638. [Accessed: 18-Aug-2024].
- [41] Robustelli, P., Piana, S., and Shaw, D. E., 2018, "Developing a Molecular Dynamics Force Field for Both Folded and Disordered Protein States," Proc Natl Acad Sci U S A, 115(21), pp. E4758–E4766. https://doi.org/10.1073/pnas.1800690115.
- [42] Ziada, S., Diharce, J., Serillon, D., Bonnet, P., and Aci-Sèche, S., 2024, "Highlighting the Major Role of Cyclin C in Cyclin-Dependent Kinase 8 Activity through Molecular Dynamics Simulations," Int J Mol Sci, 25(10). https://doi.org/10.3390/ijms25105411.
- [43] Messias, A., Santos, D. E. S., Pontes, F. J. S., Lima, F. S., and Soares, T. A., 2020, "Out of Sight, Out of Mind: The Effect of the Equilibration Protocol on the Structural Ensembles of Charged Glycolipid Bilayers," Molecules, 25(21). https://doi.org/10.3390/molecules25215120.
- [44] Kufareva, I., and Abagyan, R., 2012, "Methods of Protein Structure Comparison," Methods in Molecular Biology, 857, pp. 231–257. https://doi.org/10.1007/978-1-61779-588-6_10.
- [45] Yagnik, J., 2014, "PSPP A FREE AND OPEN SOURCE TOOL FOR DATA ANALYSIS."
- [46] Vaidya, M., Vaghela, D., Patel, Y., and Solanki, H., 2017, "R: An Open Source Software Environment for Statistical Analysis."
- [47] Goldsteint, E. J. C., Citron, D. M., and Alden, R. M., 1985, Comparative In vitro Inhibitory and Killing Activity of Cefpirome, Ceftazidime, and Cefotaxime Against Pseudomonas Aeruginosa, Enterococci, Staphylococcus Epidermidis, and Methicillin-Susceptible and Resistant and Tolerant and Nontolerant Staphylococcus Aureus.
- [48] Waterhouse, A., Bertoni, M., Bienert, S., Studer, G., Tauriello, G., Gumienny, R., Heer, F. T., de Beer, T. A. P., Rempfer, C., Bordoli, L., Lepore, R., and Schwede, T., 2018, "SWISS-MODEL: Homology Modelling of Protein Structures and Complexes," Nucleic Acids Res, 46(W1), pp. W296–W303. https://doi.org/10.1093/nar/gky427.
- [49] Edwards, J. R., 1988, "Cefotetan: Antibacterial Activity against Staphylococcus Aureus in the Presence of Human Serum.," Chemioterapia, 7(4), pp. 271–273.
- [50] Rawat, D., and Nair, D., 2010, "Extended-Spectrum β-Lactamases in Gram Negative Bacteria.," J Glob Infect Dis, 2(3), pp. 263–274. https://doi.org/10.4103/0974-777X.68531.
- [51] Hasan, M. A., Khan, M. A., Sharmin, T., Hasan Mazumder, M. H., and Chowdhury, A. S., 2016, "Identification of Putative Drug Targets in Vancomycin-Resistant Staphylococcus Aureus (VRSA) Using Computer Aided Protein Data Analysis," Gene. https://doi.org/10.1016/j.gene.2015.08.044.
- [52] Vanthida, H., and J., R. M., 2005, "Pharmacodynamics of Cefepime Alone and in Combination with Various Antimicrobials against Methicillin-Resistant Staphylococcus Aureus in an In vitro Pharmacodynamic Infection Model," Antimicrob Agents Chemother, 49(1), pp. 302–308. https://doi.org/10.1128/AAC.49.1.302-308.2005.
- [53] Paci, M., Koivumäki, J. T., Lu, H. R., Gallacher, D. J., Passini, E., and Rodriguez, B., 2021, "Comparison of the Simulated Response of Three *in Silico* Human Stem Cell-Derived Cardiomyocytes Models and In vitro Data Under 15 Drug Actions," Front Pharmacol, 12(March), pp. 1–16. https://doi.org/10.3389/fphar.2021.604713.
- [54] [Chiang, T.T., Tang, H.-J., Chiu, C.-H., Chen, T.-L., Ho, M.-W., Lee, C.-H., Sheng, W.-H., and Yang, Y.-S., 2016, "Antimicrobial Activities of Cefoperazone-Sulbactam in Comparison to Cefoperazone against Clinical Organisms from Medical Centers in Taiwan," Journal of Medical Sciences, 36(6), pp. 229–233. https://doi.org/10.4103/1011-4564.196365.
- [55] Yamachika, S., Sugihara, C., Kamai, Y., and Yamashita, M., 2013, "Correlation between Penicillin-Binding Protein 2 Mutations and Carbapenem Resistance in Escherichia Coli," J Med Microbiol, 62(3), pp. 429–436. https://doi.org/10.1099/jmm.0.051631-0.
- [56] Wiener, E. S., Heil, E. L., Hynicka, L. M., Kristie Johnson, J., Villedieu, A., Diaz-Torres, M. L., Hunt, N., McNab, R., Spratt, D. A., Wilson, M., Mullany, P., Vading, M., Nauclér, P., Kalin, M., Giske, C. G., Shulman-Peleg, A., Nussinov, R., Wolfson, H. J., Shoemaker, B. A., Zhang, D., Thangudu, R. R., Tyagi, M., Fong, J. H., Marchler-Bauer, A., Bryant, S. H., Madej, T., Panchenko, A. R., Shi, C., Xiao, Y., Zhang, Q., Li, Q., Wang, F., Wu, J., Lin, N., Ramadan, A. A., Abdelaziz, N. A., Amin, M. A., Aziz, R. K., Prasad, R., Verma, S. K., Garg, R., Jain, A., Anand, S. C., Hosmane, G. B., Verma, R. K., Kushwaha, N. S., Kant, S., Pencheva, T., Lagorce, D., Pajeva, I., Villoutreix, B. O., Miteva, M. A., Mok, S., Hannan, M. M., Nölke, L., Stapleton, P., O'Sullivan, N., Murphy, P., McLaughlin, A. M., McNamara, E., Fitzgibbon, M. M., Rogers, T. R., Malchione, M. D., Torres, L. M., Hartley, D. M., Koch, M., Goodman, J. L., Mahmood, T., Roy, S., Siddiqui, H. H., Shamim, A., Loeffler, J. M., Garbino, J., Lew, D., Harbarth, S., Rohner, P., Lim, W. W., Wu, P., Bond, H. S., Wong, J. Y.,

ISSN: 2229-7359 Vol. 11 No. 15s,2025

https://theaspd.com/index.php

Ni, K., Seto, W. H., Jit, M., Cowling, B. J., Li, Z., Wan, H., Shi, Y., Ouyang, P., Laxminarayan, R., Chaudhury, R. R., Klein, C. D., Bachelier, A., Kim, S. Y., Kim, J., Jeong, S.-I., Jahng, K. Y., Yu, K.-Y., Keynan, Y., Rubinstein, E., Jokinen, E., Laine, J., Huttunen, R., Lyytikäinen, O., Vuento, R., Vuopio, J., Syrjänen, J., Halgren, T. A., Murphy, R. B., Friesner, R. A., Beard, H. S., Frye, L. L., Pollard, W. T., Banks, J. L., Gueimonde, M., Sánchez, B., G de Los Reyes-Gavilán, C., Margolles, A., de los Reyes-Gavilán, C. G., Margolles, A., Grebe, T., Hakenbeck, R., Ghafur, A., Frieri, M., Kumar, K., Boutin, A., Day, M. J., Hopkins, K. L., Wareham, D. W., Toleman, M. A., Elviss, N., Randall, L., Teale, C., Cleary, P., Wiuff, C., Doumith, M., Ellington, M. J., Woodford, N., Livermore, D. M., Cousins, K. R., Chaurasia, M., Hussain, Z., Agha, V., Caneiras, C., Lito, L., Melo-Cristino, J., Duarte, A., C. Willyard, Bhardwaj, N., Mathur, P., Behera, B., Mathur, K., Kapil, A., Misra, M. C., Berman, H. M., Battistuz, T., Bhat, T. N., Bluhm, W. F., Bourne, P. E., Burkhardt, K., Feng, Z., Gilliland, G. L., Iype, L., Jain, S., Fagan, P., Marvin, J., Padilla, D., Ravichandran, V., Schneider, B., Thanki, N., Weissig, H., Westbrook, J. D., and Zardecki, C., 2019, "Antibiotic Resistance in Probiotic Bacteria," Int J Antimicrob Agents, 4(4), pp. 381–399. https://doi.org/10.3389/fmicb.2013.00202.

- [57] Ramadan, A. A., Abdelaziz, N. A., Amin, M. A., and Aziz, R. K., 2019, "Novel BlaCTX-M Variants and Genotype-Phenotype Correlations among Clinical Isolates of Extended Spectrum Beta Lactamase-Producing Escherichia Coli," Sci Rep, 9(1). https://doi.org/10.1038/s41598-019-39730-0.
- [58] Wicherts, J. M., Veldkamp, C. L. S., Augusteijn, H. E. M., Bakker, M., van Aert, R. C. M., and van Assen, M. A. L. M., 2016, "Degrees of Freedom in Planning, Running, Analyzing, and Reporting Psychological Studies: A Checklist to Avoid P-Hacking," Front Psychol, 7(NOV), pp. 1–12. https://doi.org/10.3389/fpsyg.2016.01832.
- [59] Ruxton, G. D., and Neuhäuser, M., 2010, "When Should We Use One-Tailed Hypothesis Testing?," Methods Ecol Evol, 1(2), pp. 114–117. https://doi.org/10.1111/j.2041-210x.2010.00014.x.
- [60] Tita, A. T. N., Thinking, O., and Restraints, E., 2002, "In Clinical Research," pp. 3062-3065. https://doi.org/10.1161/01.CIR.0000018283.15527.97.
- [61] Schober, P., Boer, C., and Schwarte, L. A., 2018, "Correlation Coefficients: Appropriate Use and Interpretation," Anesth Analg, 126(5).
- [62] Hagquist, C., and Stenbeck, M., 1998, "Goodness of Fit in Regression Analysis R2 and G2 Reconsidered," Qual Quant, 32(3), pp. 229–245. https://doi.org/10.1023/A:1004328601205.
- [63] Krzywinski, M., and Altman, N., 2014, "Visualizing Samples with Box Plots," Nat Methods, 11(2), pp. 119–120. https://doi.org/10.1038/nmeth.2813.
- [64] Nahm, F. S., 2016, "Nonparametric Statistical Tests for the Continuous Data: The Basic Concept and the Practical Use.," Korean J Anesthesiol, 69(1), pp. 8–14. https://doi.org/10.4097/kjae.2016.69.1.8.
- [65] Maruyama, Y., Igarashi, R., Ushiku, Y., and Mitsutake, A., 2023, "Analysis of Protein Folding Simulation with Moving Root Mean Square Deviation," J Chem Inf Model, 63(5), pp. 1529–1541. https://doi.org/10.1021/acs.jcim.2c01444.
- [66] Jia, P., Zhu, Y., Zhang, H., Cheng, B., Guo, P., Xu, Y., and Yang, Q., 2022, "In vitro Activity of Ceftaroline, Ceftazidime-Avibactam, and Comparators against Gram-Positive and -Negative Organisms in China: The 2018 Results from the ATLAS Program," BMC Microbiol, 22(1). https://doi.org/10.1186/s12866-022-02644-5.
- [67] Truong, D. T., Ho, K., Pham, D. Q. H., Chwastyk, M., Nguyen-Minh, T., and Nguyen, M. T., 2024, "Treatment of Flexibility of Protein Backbone in Simulations of Protein-Ligand Interactions Using Steered Molecular Dynamics," Sci Rep, 14(1). https://doi.org/10.1038/s41598-024-59899-3.
- [68] Lowy, F. D., 2003, "Antimicrobial Resistance: The Example of Staphylococcus Aureus," Journal of Clinical Investigation, 111(9), pp. 1265–1273. https://doi.org/10.1172/jci200318535.
- [69] Rampogu, S., Lee, G., Park, J. S., Lee, K. W., and Kim, M. O., 2022, "Molecular Docking and Molecular Dynamics Simulations Discover Curcumin Analogue as a Plausible Dual Inhibitor for SARS-CoV-2," Int J Mol Sci, 23(3). https://doi.org/10.3390/ijms23031771.
- [70] Bagewadi, Z. K., Yunus Khan, T. M., Gangadharappa, B., Kamalapurkar, A., Mohamed Shamsudeen, S., and Yaraguppi, D. A., 2023, "Molecular Dynamics and Simulation Analysis against Superoxide Dismutase (SOD) Target of Micrococcus Luteus with Secondary Metabolites from Bacillus Licheniformis Recognized by Genome Mining Approach," Saudi J Biol Sci, 30(9). https://doi.org/10.1016/j.sjbs.2023.103753.
- [71] Zhang, K., Zhang, C., Teng, X., Wang, K., and Chen, M., 2023, "Bioinformatics and Computational Chemistry Approaches to Explore the Mechanism of the Anti-Depressive Effect of Ligustilide," Sci Rep, 13(1). https://doi.org/10.1038/s41598-023-32495-7.
- [72] Nada, H., Elkamhawy, A., and Lee, K., 2022, "Identification of 1H-Purine-2, 6-Dione Derivative as a Potential SARS-CoV-2 Main Protease Inhibitor: Molecular Docking, Dynamic Simulations, and Energy Calculations," PeerJ, 10. https://doi.org/10.7717/peerj.14120.